



GLACIAL/INTERGLACIAL CHANGES IN MINERAL DUST AND SEA-SALT RECORDS IN POLAR ICE CORES: SOURCES, TRANSPORT, AND DEPOSITION

Hubertus Fischer,¹ Marie-Louise Siggaard-Andersen,^{1,2} Urs Ruth,¹ Regine Röthlisberger,³ and Eric Wolff³

Received 13 December 2005; accepted 18 October 2006; published 24 February 2007.

[1] Sea-salt and mineral dust records as represented by Na^+ and Ca^{2+} concentrations, respectively, in Greenland and Antarctic ice cores show pronounced glacial/interglacial variations. For the Last Glacial Maximum (LGM), mineral dust (sea salt) concentrations in Greenland show an increase of a factor of approximately 80 (15) compared to the Holocene and significant shifts by a factor of 15 (5) during Dansgaard-Oeschger events. In Antarctica the dust (sea salt) flux is enhanced by a factor of 15 (3) during the LGM compared to the Holocene, and variations by approximately a factor of 8 (1–2) exist in parallel to Antarctic warm events. Primary glacial dust sources are the Asian deserts for Greenland and Patagonia for Antarctica. Ice core evidence and model results show that both changes

in source strength as well as atmospheric transport and lifetime contributed to the observed changes in Greenland ice cores. In Antarctica, changes in ice core fluxes are in large parts related to source variations both for sea salt and dust, where the formation of sea-salt aerosol from sea ice may play a pivotal role. Summarizing our latest estimates on changes in sources, transport, and deposition, these processes are roughly able to explain the glacial increase in sea salt in both polar regions, while they fall short by at least a factor of 4–7 for mineral dust. Future improvements in model resolution and in the formulation of source and transport processes together with new ice core records, e.g., on dust size distributions, will eventually allow convergence of models and observations.

Citation: Fischer, H., M.-L. Siggaard-Andersen, U. Ruth, R. Röthlisberger, and E. Wolff (2007), Glacial/interglacial changes in mineral dust and sea-salt records in polar ice cores: Sources, transport, and deposition, *Rev. Geophys.*, 45, RG1002, doi:10.1029/2005RG000192.

1. INTRODUCTION

[2] Atmospheric aerosol plays an important role both in global biogeochemical cycles and in the climate system of the Earth. Long-range aerosol transport enables the export of nutrients to and across the oceans, the latter being crucial for the bioproductivity in remote regions [Boyd *et al.*, 2000; Falkowski *et al.*, 2000; Martin, 1990; Swap *et al.*, 1992; Watson *et al.*, 2000]. Aerosols also affect the radiative balance of the Earth [Tegen *et al.*, 1996] directly by scattering or absorption of incoming shortwave radiation and indirectly by acting as cloud condensation nuclei, altering a temperature effect at the surface because of changes in cloud cover [Intergovernmental Panel on Climate Change, 2001]. In addition, aerosol particles are intimately coupled to atmospheric chemistry as chemical

reactions in the atmosphere are often accelerated on aerosol surfaces [Dentener *et al.*, 1996] providing water, oxidants, and/or catalysts.

[3] Besides this active role in the Earth system, sea-salt and mineral dust aerosol, which are conservatively archived in polar ice cores, represent passive tracers that can be used to reconstruct climate conditions in their source regions as well as large-scale atmospheric transport patterns. The life cycle of an aerosol particle starts with its formation. In the case of sea salt, aerosol production is caused by wind dispersion of seawater in liquid and frozen state. Dispersion of wave crests and the bursting of small air bubbles at the ocean surface producing small droplets [Monahan *et al.*, 1986] represent an efficient way of producing sea-salt particles, which may be uplifted by convective cells in the boundary layer. In high latitudes, sea-salt aerosol additionally derives from the sea ice surface. For example, frost flowers, which form during the refreezing of polynyas and open leads within the sea ice cover, allow for the entrainment of sea-salt particles into the atmosphere [Rankin *et al.*, 2000; Wagenbach *et al.*, 1998]. In the case of mineral dust,

¹Alfred Wegener Institute for Polar and Marine Research, Bremerhaven, Germany.

²Now at Niels Bohr Institute, University of Copenhagen, Copenhagen, Denmark.

³British Antarctic Survey, Cambridge, UK.

chemical and physical weathering of crustal material leads to the formation of small dust particles that may get entrained into the air during high surface winds. Larger particles may be horizontally accelerated by surface wind and collide with other particles, an avalanche process called saltation [Marticorena and Bergametti, 1995]. The impact is able to provide vertical momentum to the smaller particles and leads to entrainment into the boundary layer and subsequently efficient uplift by convection.

[4] The sea-salt and mineral dust load in the atmosphere is strongly influenced by the climate conditions in the source region, and aerosol records provide information, e.g., on cyclonic activity and wind speeds and, in the case of dust, on soil properties such as aridity [Genthon, 1992] or vegetation cover. In the case of the mineral dust sources, which are located in arid and semiarid regions in both hemispheres far away from the polar ice sheets [Prospero et al., 2002], dust storm events provide the energy to lift dust particles to the high troposphere above the cloud level, where their atmospheric lifetime is large enough to survive long-range transport [Gong et al., 2003; Prospero et al., 2002; Sun, 2002; Tegen, 2003]. Sea-salt aerosol formation is closely linked to cyclonic activity, providing high wind speeds on the ocean surface for efficient sea-salt aerosol formation. Sea-salt aerosol is then also efficiently transported and mainly wet deposited along the storm track [Fischer and Mieding, 2005; Fischer et al., 2004]. It follows that sea-salt and snow deposition is closely linked in regions of ice sheets where intrusions of marine air masses and frontal precipitation occur.

[5] The long-range transported aerosol is wet and dry deposited onto the ice sheets, where a stratigraphically ordered sequence of precipitation and aerosol deposition events is formed. Accordingly, ice core records retrieved from the polar ice sheets on both hemispheres (Figure 1) provide aerosol records in high (in some cases seasonal) resolution over the last glacial/interglacial cycles. The major feature of these records is a 1–2 orders of magnitude increase in sea-salt aerosol and mineral dust concentration during glacial periods. The reasons for this change have still not been quantitatively explained and may be sought in the three steps of the aerosol life cycle: production, transport, and deposition, or any combination of the three. Accordingly, different hypotheses have been put forward in the literature based on observational, theoretical, and modeling evidence to explain the documented changes. In this study we will summarize the observational and modeling evidence, discuss the different hypotheses, and try to come up with a synthesis and explanation of the glacial/interglacial changes in sea-salt and mineral dust concentrations in ice cores.

[6] This review is organized in five sections. In section 2 the results concerning sea-salt and mineral dust records from major ice core projects in Greenland and Antarctica are summarized. Section 2 presents the database that has to be explained in terms of changes in the geochemical aerosol cycles over glacial/interglacial timescales. We intentionally restrict the discussion to a few ice cores representative of the two major ice sheets, because those are distal to any local

aerosol sources and therefore are most likely to archive changes in background aerosol concentrations for each hemisphere. Valuable information on dust emissions may also be derived from tropical ice core records [Thompson et al., 1995, 1997, 1998]; however, those cores reflect mainly local conditions of dust generation, uplift, and transport. Section 3 discusses the contribution of processes that may have led to the observed long-term changes based on ice core evidence and theoretical considerations. In sections 3.1–3.3, possible changes in the three stages of an aerosol lifetime are individually discussed. Because the understanding of aerosol deposition is a fundamental prerequisite for the interpretation of ice core records, we will discuss the individual processes in reverse order of the aerosol life cycle, i.e., starting with the deposition of aerosol on the ice sheets in section 3.1. Then we will quantify transport changes in section 3.2, and finally, we discuss potential emission changes in section 3.3, where uncertainties are still large because quantitative observational evidence is sparse. In section 4 we tackle this question from a different direction by contrasting the observational evidence in section 3 with a summary of the current state of the art in global modeling of aerosol emission and transport. This may give additional insight into the potential of individual processes to contribute to the glacial/interglacial aerosol changes but will also show the limitations of aerosol modeling that still exist to date. In section 5 we attempt a quantitative synthesis of the state of the art of our knowledge on sea-salt and mineral dust aerosol changes as recorded in ice cores as summarized in Table 1; we point out gaps in our knowledge and suggest future directions in ice core and modeling studies to fill those gaps.

2. CONTINUOUS AEROSOL RECORDS IN GREENLAND AND ANTARCTICA

2.1. Methods and Uncertainties

[7] Sea salt and mineral dust aerosol are transported onto the polar ice sheets, where they are archived by wet and dry deposition. Using snow and ice core samples, concentrations and size distributions of particulate dust can be determined using particle counting techniques [Delmonte et al., 2002; Petit et al., 1990; Ram and Koenig, 1997; Ruth et al., 2003; Steffensen, 1985]. Specific soluble dust tracers (e.g., Ca^{2+}) or insoluble elements contained in particulate dust (e.g., Al and Fe) as well as ionic species derived from sea salt (mainly, Na^+ and Cl^-) are also conveniently used to quantify aerosol changes. Ionic and elemental concentrations are determined, for example, by ion chromatography (IC), atomic absorption spectroscopy, inductively coupled plasma mass spectrometry, or continuous flow analyses (CFA) [Boutron, 1979; Fischer and Wagenbach, 1996; Fuhrer et al., 1993; Gabrielli et al., 2005; Mayewski et al., 1987; Röthlisberger et al., 2000; Steffensen, 1988]. A detailed description of these analytical techniques, handling of ultraclean ice core samples, and the systematic and stochastic error of such measurements is beyond the scope of this paper. Here we will focus mainly on soluble species

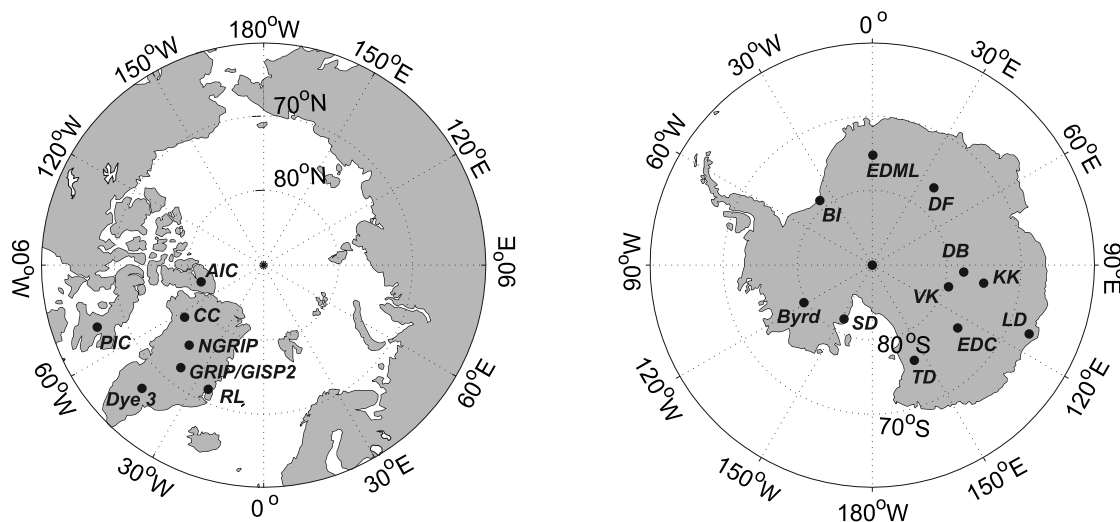


Figure 1. Map of both polar regions showing major ice core drilling sites in the Arctic (AIC, Agassiz Ice Cap; PIC, Penny Ice Cap; CC, Camp Century; NGRIP; GRIP/GISP2; RL, Renland; and Dye 3) and in Antarctica (EDML, EPICA Dronning Maud Land; BI, Berkner Island; DF, Dome Fuji; VK, Vostok; DB, Dome B; KK, Komsomolskaya; Byrd; SD, Siple Dome; TD, Taylor Dome; EDC, EPICA Dome C; and LD, Law Dome).

representing sea-salt (Na^+) and mineral dust (Ca^{2+}) aerosol that can be determined by IC and CFA with an error typically better than 10% for concentrations above the blank level (typically a few parts per billion) and where the available database to date is better than for other dust indicators. Note that Ca^{2+} is, in principle, only representative of part of the overall dust content in the ice, but by and large, both particulate dust and the soluble dust proxy Ca^{2+} reveal the same picture of paleoclimatic changes in the dust cycle (Table 1). A recent comparison of soluble Ca^{2+} with the total Ca^{2+} concentration derived by complete acid digestion of ice core samples from Dome C, Antarctica, showed that the soluble Ca^{2+} amount varied between 80 and 90% of the total Ca^{2+} level for glacial and interglacial samples (V. Gaspari, personal communication, 2006). This variability is much lower than the glacial/interglacial variability found in the ice cores and can therefore be neglected to first order.

[8] Aerosol deposition fluxes are derived by multiplying ice core concentrations by the annual snow accumulation rate. In general, accumulation rates are reduced during cold climate conditions, resulting in smaller glacial/interglacial variations in estimated fluxes than in measured concentrations. Snow accumulation rates can be determined at high-resolution sites by counting annual layers, for example, in high-resolution CFA profiles, and destraining the layers, which have been subject to down-core thinning due to glacier flow, using an ice flow model [Cuffey and Clow, 1997]. In low-accumulation areas, as largely encountered in the interior of East Antarctica, individual annual layers cannot be resolved. Here the accumulation rate is usually estimated from temperature reconstructions derived from the stable water isotope composition ($\delta^{18}\text{O}$ or δD). In short, the accumulation is assumed to be thermodynamically controlled by the change in saturation water vapor pressure, which is a function of temperature (see supplemental material of *EPICA Community Members* [2004] and

Schwander et al. [2001]). The error of such accumulation rates can be estimated to be 20–30%. Accordingly, the error in aerosol fluxes is about 30%. Although considerable, this uncertainty is still small compared to the changes in sea salt and dust encountered on millennial timescales in the glacial period and during glacial/interglacial transitions. Accordingly, analytical limitations generally do not affect the conclusions drawn in this study.

2.2. Sea-Salt and Mineral Dust Budget in Both Polar Regions

[9] Average concentrations in Greenland and Antarctica reflect the different setting of the Earth's two major ice sheets. Antarctica is surrounded by the Southern Ocean as reflected by much higher sea-salt concentrations and fluxes compared to mineral dust. For recent conditions the number

TABLE 1. Ratios of Observed Mineral Dust and Sea-Salt Parameters in Ice Cores Between the LGM and the Holocene as Well as Between Stadial and Interstadial Periods^a

Parameter	Ice Core	LGM/Holocene	S/IS
<i>Greenland</i>			
Ca^{2+} concentration	GISP2	~80	15–20
Particulate dust concentration	NGRIP	80–100	~15
Na^+ concentration	GISP2	10–15	4–5
Ca^{2+} flux	GISP2	15–20	6–10
Particulate dust flux	NGRIP	~20	~8
Na^+ flux	GISP2	3–4	2–3
<i>Antarctica</i>			
Ca^{2+} concentration	EDC	25–30	
Particulate dust concentration	Vostok	30–35	
Na^+ concentration	EDC	~5	
Ca^{2+} flux	EDC	10–15	
Particulate dust flux	Vostok	~15	
Na^+ flux	EDC	~3	

^aAbbreviations are LGM, Last Glacial Maximum; Greenland Ice Sheet Project 2, GISP2; North Greenland Ice Core Project, NGRIP; EDC, EPICA Dome C; S, stadial; and IS, interstadial.

of Na^+ molecules per kilogram of ice in Antarctica is a factor of 25 higher than that for Ca^{2+} [Petit et al., 1999; Wolff et al., 2006], while in Greenland it is only twice as high. In the Last Glacial Maximum (LGM) the number of Na^+ molecules per kilogram ice is still about 4 times higher than that for Ca^{2+} in Antarctica [Petit et al., 1999; Wolff et al., 2006], while it is even a factor of 2 lower in Greenland [Mayewski et al., 1994], reflecting the relatively higher influence of continental aerosol in Greenland. Also, the temporal evolution of mineral dust and sea-salt aerosol is quite different for both polar regions and reflects the different climate evolution in the Northern and Southern hemispheres as documented in ice core aerosol records from Greenland and Antarctica (e.g., Dye 3 [Hammer et al., 1985], Greenland Ice Core Project (GRIP) [de Angelis et al., 1997; Fuhrer et al., 1999], Greenland Ice Sheet Project 2 (GISP2) [Mayewski et al., 1994, 1997; Taylor et al., 1997], Renland [Hansson, 1994], Vostok [de Angelis et al., 1992; Petit et al., 1999], Taylor Dome [Mayewski et al., 1996], and the European Project for Ice Coring in Antarctica (EPICA) Dome C [Röthlisberger et al., 2002; Wolff et al., 2006]).

[10] Although measured Na^+ and Ca^{2+} concentrations can generally be taken as sea-salt and dust tracers, respectively, a crustal contribution to Na^+ may be possible, and some Ca^{2+} is derived from seawater. This has to be considered, for example, when performing correlation analyses between the two records (section 3.2), and can, in principle, be corrected for using average $\text{Na}^+/\text{Ca}^{2+}$ ratios in seawater and crustal material. For Greenland the Cl^-/Na^+ ratio in the ice cores is very close to the seawater ratio during glacial times [Mayewski et al., 1994, 1997], and during the Holocene a Cl^- excess prevails, which has been related to the longer atmospheric lifetime of gaseous HCl released from sea-salt aerosol [Legrand et al., 2002; Legrand and Delmas, 1988] in an acidic atmosphere. This indicates that, with the exception of particular dust events, Na^+ is essentially of sea-salt origin in Greenland. The sea-salt contribution to Ca^{2+} estimated using the seawater $\text{Ca}^{2+}/\text{Na}^+$ ratio is only around 10% during the Holocene and is much lower during glacial times. Therefore we refrain from correcting Na^+ and Ca^{2+} concentrations in Greenland for their crustal and sea-salt contributions, respectively.

[11] On the East Antarctic plateau the seawater contribution to Ca^{2+} is high for the Holocene (around 50%), while crustal Na^+ becomes important during the glacial period (20–30% of the total Na^+ concentration). In that case, non-sea-salt Ca^{2+} (nss Ca^{2+}) and sea-salt Na^+ (ss Na^+) can be estimated [Röthlisberger et al., 2002] according to

$$\text{nssCa}^{2+} = \frac{R_t}{R_t - R_m} (\text{Ca}^{2+} - R_m \text{Na}^+)$$

$$\text{ssNa}^+ = \text{Na}^+ - \frac{1}{R_t - R_m} (\text{Ca}^{2+} - R_m \text{Na}^+),$$

with $R_m = 0.038$ (in mass concentration units) being the $\text{Ca}^{2+}/\text{Na}^+$ seawater ratio, which is well defined globally. $R_t \approx 1.78$ [Bowen, 1979] represents the crustal ratio, which varies over a wide range, dependent on the composition of crustal material as well as on size-dependent fractionation processes of different minerals during the formation of

mineral dust aerosol. In addition, the composition of crustal tracers as recorded in ionic ice core data may differ from R_t , which is based on the total elemental composition of crustal material. While the effect of such a variability in R_t changes the nss Ca^{2+} estimate only by a few percent, its effect on ss Na^+ is considerable. For instance, reducing R_t within reasonable bounds to 1.1 [Bigler et al., 2006] or increasing it to 3.5 changes the ss Na^+ estimate by 10–30% for glacial conditions in Antarctica.

2.3. Temporal Changes Over the Last Glacial Cycles

[12] In Figure 2 the Na^+ and Ca^{2+} record of the GISP2 ice core [Mayewski et al., 1994] is shown, together with $\delta^{18}\text{O}$ [Grootes et al., 1993] taken as representative for climate changes at least in the northern Atlantic region [Bond et al., 1993; McManus et al., 1999; Porter and An, 1995; Schulz et al., 1998]. As illustrated in Figure 2, both sea salt (Na^+) and mineral dust (Ca^{2+}) are strongly anticorrelated with Greenland temperature changes, including rapid climate changes such as the warming at the end of the Younger Dryas [Dansgaard et al., 1989; Taylor et al., 1997] or each individual Dansgaard-Oeschger (DO) event [Fuhrer et al., 1999; Grootes et al., 1993; Johnsen et al., 1992; Mayewski et al., 1994]. Na^+ concentrations during the LGM are, on average, 10–15 times higher than during the Holocene, while Ca^{2+} was increased by a factor of approximately 80. Extreme steps in aerosol concentrations are encountered at the end of the Younger Dryas (YD) to the Preboreal (PB) where Na^+ and Ca^{2+} concentrations drop in only a few decades by a factor of about 4 and 8, respectively. Taking the concurrent change in snow accumulation [Cuffey and Clow, 1997; Meese et al., 1994] into account, deposition fluxes in the LGM were a factor of 3–4 and 15–20 higher than during the Holocene for Na^+ and Ca^{2+} , respectively. For the shift from the YD to the PB this leads to a decline in fluxes by a factor of approximately 2 and 4, respectively. A similar instantaneous response holds for the DO events during marine isotope stage (MIS) 3. Here sea-salt concentrations decrease rapidly from cold stadials (S) to warm interstadials (IS) by a factor of 4–5, and mineral dust concentrations decrease by a factor of 15–20. Fluxes change at the same time by a factor of 2–3 and 6–10 for sea salt and dust, respectively.

[13] In principle, a similar picture emerges for the changes in aerosol concentration in Antarctica with higher concentrations during cold and lower concentrations during warm periods. For example, from the LGM to the Holocene, Na^+ concentrations in the Vostok record [Petit et al., 1999] decrease by about a factor of 4, and particulate dust concentrations decrease by a factor of 30–35 (Figure 3). Although rapid climate changes are not encountered in the Southern Hemisphere, high-resolution chemistry records from the EPICA Dome C (EDC) ice core [Röthlisberger et al., 2002; Wolff et al., 2006] show that more gradual variations in Ca^{2+} concentrations are found on a millennial timescale. As shown in Figure 4, the Antarctic warm event A1 (representing the Antarctic counterpart to DO event 8 [Blunier et al., 1998; Broecker, 1998; Knutti et al., 2004; Stocker and

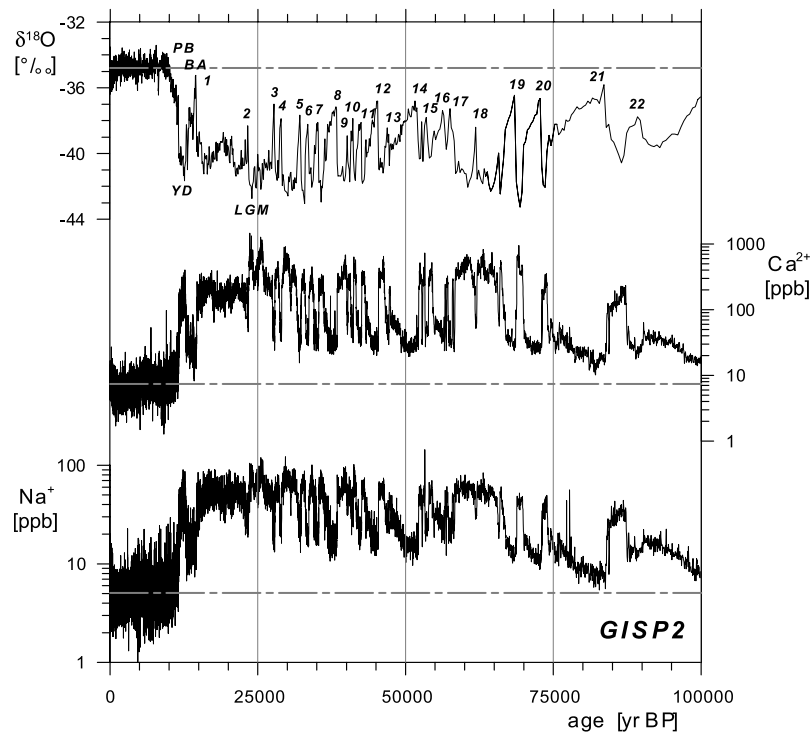


Figure 2. Temporal evolution of $\delta^{18}\text{O}$ indicating changes in average local condensation temperature during snow formation, the mineral dust component Ca^{2+} , and the sea-salt component Na^+ over the last glacial cycle as recorded in the central Greenland GISP 2 ice core [Grootes et al., 1993; Mayewski et al., 1997, 1994]. Also marked are the Preboreal (PB) period and the Last Glacial Maximum (LGM) as well as rapid climate events such as the Younger Dryas (YD), the Bølling/Allerød Oscillation (BA), and the Dansgaard-Oeschger events 1–22. Dashed-dotted lines indicate Holocene levels.

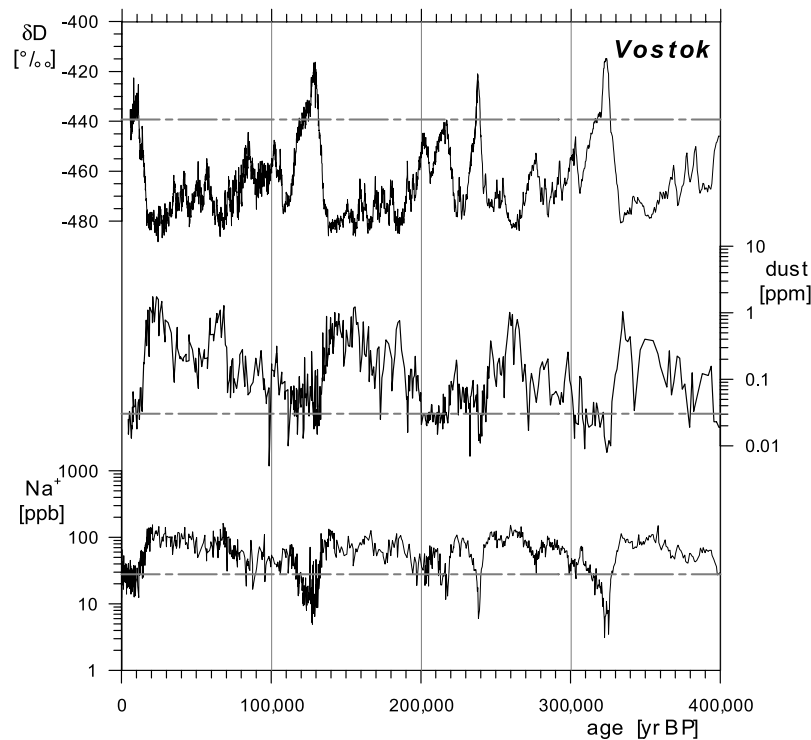


Figure 3. Temporal evolution of δD representing changes in the average local condensation temperature during snow formation, the particulate dust, and the sea-salt component Na^+ over the last four glacial cycles as recorded in the East Antarctic Vostok ice core [Petit et al., 1999]. Dashed-dotted lines indicate the mean Holocene level from 0 to 10,000 years B.P.

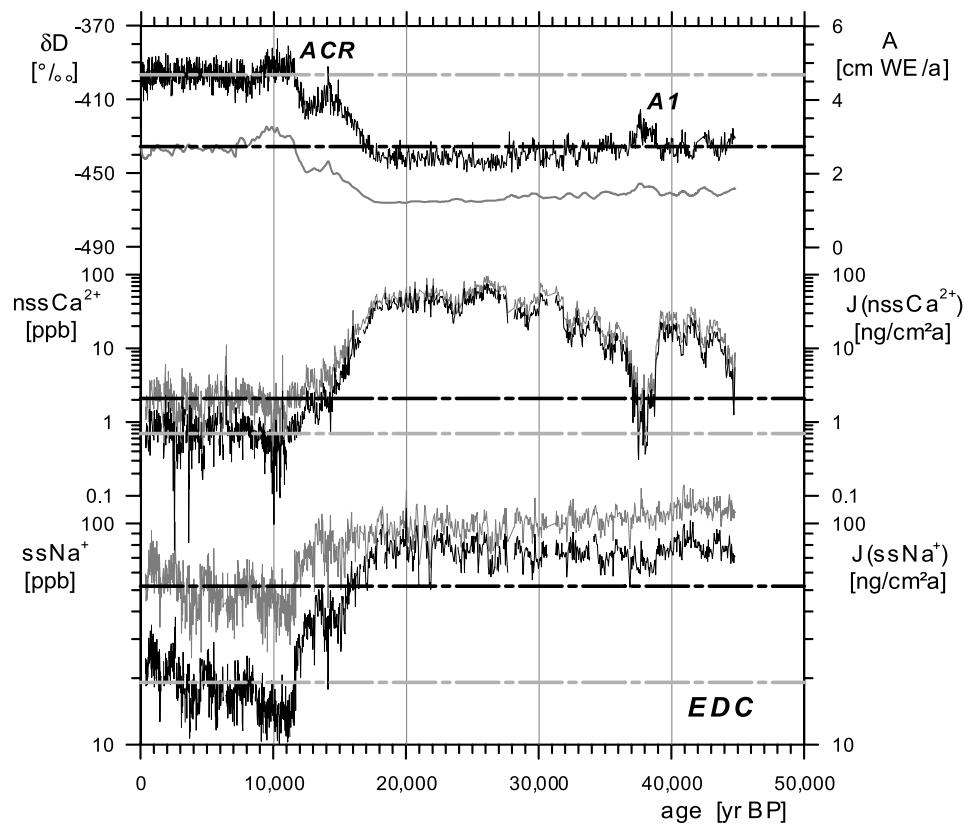


Figure 4. Comparison of concentrations (left axes) (thin black lines) and fluxes (right axes) (thin shaded lines) of sea salt (ssNa^+) and mineral dust (nssCa^{2+}) in the EDC ice core over the last 45,000 years [Röthlisberger et al., 2002] in high temporal resolution. Also given are the changes in δD (left axis) (thick black line) representing a proxy for the average local condensation temperature during snow formation and in the snow accumulation A (right axis) (thick shaded line) as described in the text. Dashed-dotted lines indicate Holocene levels. A1 indicates the Antarctic warm event 1 [Blunier and Brook, 2001; Blunier et al., 1998]; ACR indicates the Antarctic Cold Reversal [Blunier et al., 1997].

Johnsen, 2003; EPICA Community Members, 2006]) was accompanied by a decline in dust to close to Holocene levels, while the temperature proxy δD rose by about 15‰ in Figure 4 (equivalent to a surface temperature change in Antarctica of 2° – 2.5°C) [Röthlisberger et al., 2002; Stenni et al., 2001]. In contrast, sea-salt concentrations were only weakly affected by this warm event. Vice versa the Antarctic Cold Reversal (see Figure 4) is only weakly seen in the dust record but clearly imprinted in the sea-salt record. Accordingly, different causes may lead to the changes in the aerosol budget over the Antarctic ice sheet for both events. The decrease in snow accumulation in Antarctica during the glacial compared to the interglacial [Schwander et al., 2001] leads to a reduced change in deposition flux for both aerosol components (Figure 4) [Röthlisberger et al., 2002]. Over the last glacial/interglacial transition the Na^+ flux decreases by a factor of approximately 2.5, while the Ca^{2+} flux decreases by a factor of 10–15 compared to a factor of 25–30 for Ca^{2+} concentrations.

[14] On a longer timescale the Vostok record [Petit et al., 1999] shows that dust and sea salt varied within rather well constrained glacial/interglacial bounds over the last four glacial cycles (Figure 3). With the new sea-salt and dust records from the EPICA Dome C ice core [Wolff et al., 2006] this view can be extended over the four previous

glacial cycles (Figure 5), which are characterized by significantly lower glacial/interglacial temperature amplitudes in the Southern Ocean region [EPICA Community Members, 2004]. The glacial/interglacial amplitudes in aerosol fluxes are smaller for the time period 400,000–800,000 years B.P., but the relationship of aerosol fluxes and Southern Ocean temperature changes remains essentially the same (Figure 6). The early interglacials are especially characterized by higher aerosol fluxes. During the first four glacial cycles (800–400 kyr B.P.) in Figure 6a, there is a tendency to somewhat higher dust fluxes for comparable δD values than in the last four glacial cycles [Wolff et al., 2006]. In the case of sea-salt fluxes a rather linear relationship with δD is revealed (Figure 6b), indicating a very close relationship of Southern Ocean sea-salt sources and temperature (see also 3.3).

3. ICE CORE EVIDENCE OF DEPOSITION, TRANSPORT, AND EMISSION CHANGES

3.1. Local Deposition Changes

3.1.1. Theoretical Considerations

[15] Sea-salt and mineral dust aerosol is transferred from the air to the ice sheet surface by wet and dry deposition. Accordingly, any temporal change in the deposition pro-

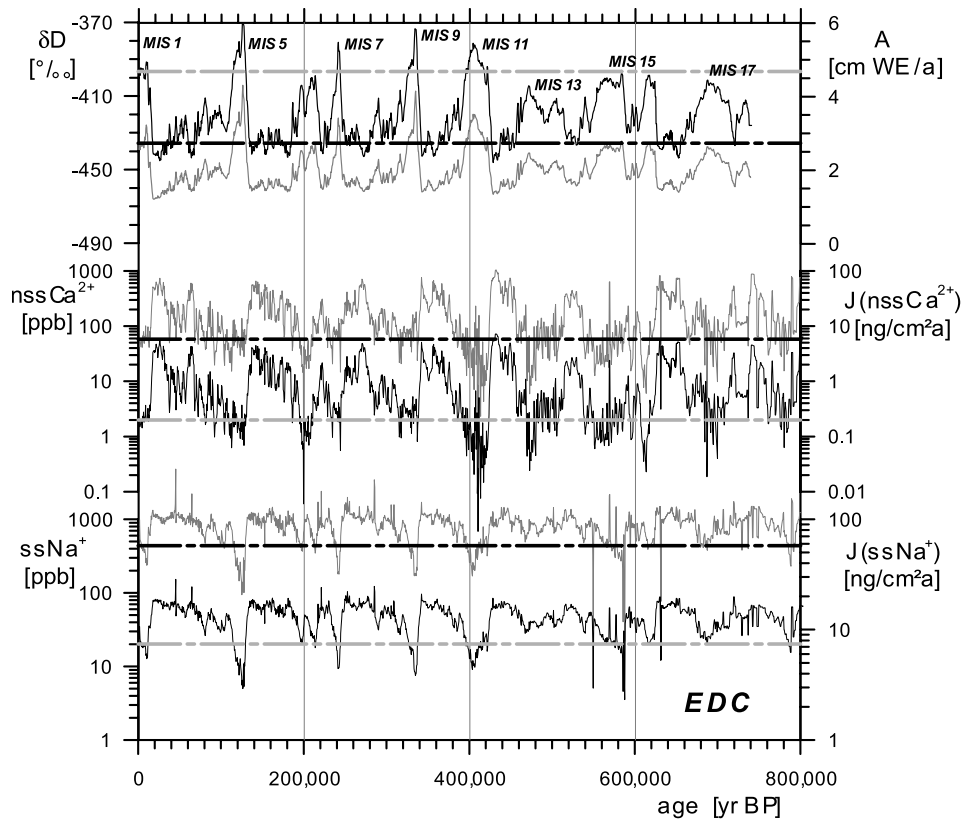


Figure 5. Comparison of concentrations (left axes) (thin black lines) and fluxes (right axes) (thin shaded lines) of sea salt ($ssNa^+$) and mineral dust ($nssCa^{2+}$) in the EDC ice core over the last 800,000 years [Wolff et al., 2006]. Also given are the changes in δD (left axis) (thick black line) representing a proxy for the average local condensation temperature during snow formation and in the snow accumulation A (right axis) (thick shaded line) as described in the text [EPICA Community Members, 2004]. Dashed-dotted lines indicate Holocene levels. Also indicated are marine isotope stages (MIS) for interglacials.

cesses may also lead to a change in ice core concentrations and fluxes even if atmospheric concentrations were to stay constant. While dry deposition is independent of precipitation, wet deposition is proportional to the snow accumulation. Because the average snow accumulation A has changed between cold and warm climate periods, so has the aerosol deposition rate. In a simplified model the total

deposition flux to the ice surface $J_{ice} = C_{ice}A$ averaged over long periods can be written as [Fischer et al., 1998a]

$$J_{ice} = J_{dry} + J_{wet} = v_{dry}C_{air} + \varepsilon AC_{air}, \quad (1)$$

and therefore the average ice concentration C_{ice} can be written as

$$C_{ice} = \frac{v_{dry}}{A}C_{air} + \varepsilon C_{air}, \quad (2)$$

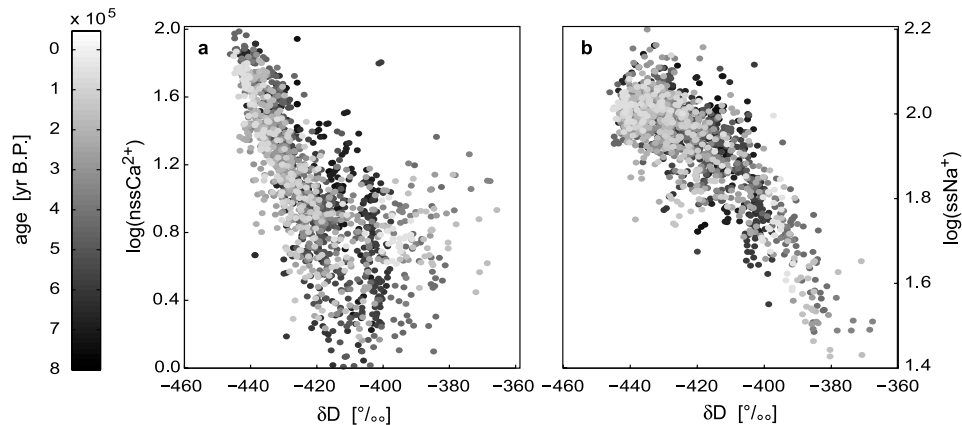


Figure 6. Time scatterplot of mineral (a) dust and (b) sea-salt fluxes in 500 year resolution in the EDC ice core [Wolff et al., 2006]. The shaded bar indicates the age of the sample.

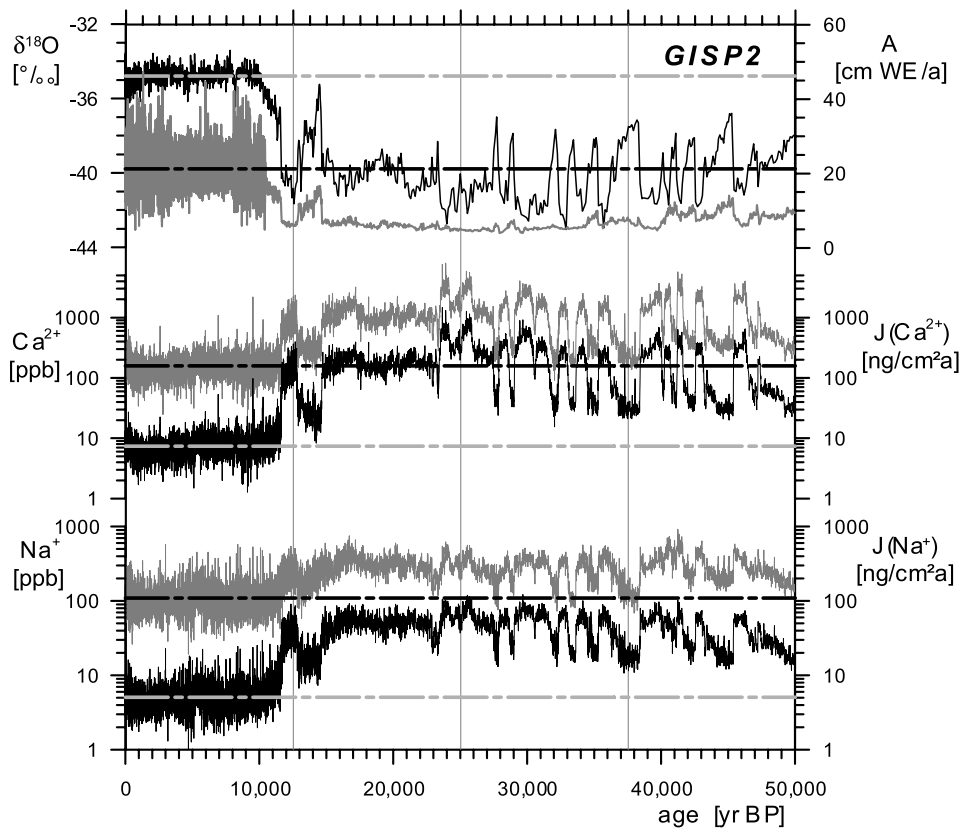


Figure 7. Comparison of concentrations (left axes) (thin black lines) and fluxes (right axes) (thin shaded lines) of sea salt (Na^+) and mineral dust (Ca^{2+}) in the GISP2 ice core record over the last 50,000 years [Mayewski et al., 1994, 1997]. Also given are the changes in $\delta^{18}\text{O}$ (left axis) (thick black line) representing a proxy for the average local condensation temperature during snow formation and the snow accumulation A (right axis) (thick shaded line). Note that the higher accumulation variability in the Holocene compared to the glacial reflects only the higher resolution of the data set as provided by Cuffey and Clow [1997]. Dashed-dotted lines indicate Holocene levels.

where v_{dry} is the effective dry deposition velocity and ε is the effective scavenging efficiency including in-cloud and below-cloud scavenging. These equations imply that in regions where wet deposition provides significant parts of the total deposition the total aerosol deposition becomes smaller in times of lower snow accumulation rates, even if all other parameters were to remain constant. Effectively, this implies that the deposition flux underestimates the changes in atmospheric concentration C_{air} overlying the ice sheet. On the contrary, C_{ice} is linearly coupled to the inverse accumulation rate and overestimates the change in C_{air} .

3.1.2. Aerosol Deposition in Greenland

[16] Greenland snow accumulation rates have been reconstructed over the last 50,000 years using the GISP2 counted depth scale [Alley et al., 1993; Meese et al., 1994] and destraining the counted annual layers, which are thinned by glacier flow. The thinning function has been determined using a glaciological flow model for three different scenarios of ice margin retreat [Cuffey and Clow, 1997]. Here we use the medium scenario, invoking a retreat of the ice sheet margin by 100 km; however, the choice of the scenario has an effect of only a few percent on the estimated snow accumulation and does not affect our conclusions. Figure 7 shows that the snow accumulation

rate during the LGM was only about 25% of the Holocene value, and accumulation rates during interstadial events were about 50% of the Holocene or twice the LGM value. Accordingly, the amplitude of flux changes of sea salt and mineral dust onto the ice is smaller than that of concentration changes in the ice. Nevertheless, fluxes and concentration are both strongly increased for cold periods, which cannot be explained by changes in the deposition efficiency over the ice sheet.

[17] Using equations (1) and (2), Alley et al. [1995] estimated the change in C_{air} for different aerosol species using the joint information of the slope and y intercept in the linear relationship between total fluxes and snow accumulation for the YD to PB period in the GISP2 record. Using this analysis, they arrive at 3 times higher air concentrations over Greenland for sea salt (here Cl^-) and 7 times higher air concentrations for Ca^{2+} during the YD compared to the PB. These values lie between the changes derived directly from flux and concentration records in the ice and imply that fluxes underestimate the change in true atmospheric concentration in central Greenland by a factor of 1.5–2, while concentrations overestimate it by only 10–30% for these species. In any case, local deposition changes can neither explain the substantial changes in concentrations nor

in fluxes over the last glacial cycle. Following the modest overestimation as supported by the results of *Alley et al.* [1995], we will discuss ice concentration, when we are interested in air concentrations over the Greenland ice sheet.

3.1.3. Aerosol Deposition in Antarctica

[18] For East Antarctic ice core drill sites such as Vostok or the EPICA drill site at Dome C the data are easier to interpret. Here recent accumulation rates are as low as 2–3 cm water equivalent/yr. Convective frontal precipitation events are unlikely, and clear-sky precipitation (diamond dust) prevails. Thus dry deposition dominates the transfer of aerosol to the ice surface under recent conditions and even more so for the lower accumulation rates encountered during glacial periods [*Legrand, 1987*]. Recent studies on aerosol distribution in ice cores from the plateau area in Dronning Maud Land, Antarctica, where accumulation rates are 2–3 times higher than at EDC, revealed that about 75% of the sulfate aerosol is dry deposited [*Göktas et al., 2002*]. A similar contribution should also apply for dust aerosol, showing that dry deposition dominates even in this area. For EDC this implies that the wet deposition term on the right-hand side of equation (1) can be neglected to first order, and conventionally, the total deposition flux is taken as a measure of the atmospheric aerosol concentration overlying the East Antarctic plateau [*Wolff et al., 2006*]. For the EDC core, accumulation rates were derived from the δD record, representing the temperature of snow formation at the cloud level (see *Schwander et al. [2001]* and supplemental material of *EPICA Community Members [2004]*). Sea-salt and mineral dust species have been measured on the EDC ice core over the last 45,000 years at high resolution using CFA [*Röthlisberger et al., 2000*] (Figure 4) and at lower resolution over the last 800,000 years by IC [*Wolff et al., 2006*]. As was the case for Greenland, both fluxes as well as concentrations change in accord, showing that the strong glacial/interglacial changes in both parameters cannot be explained by local deposition effects. In contrast to Greenland, however, the changes in fluxes can be taken as representative of changes in air concentration, while the ice concentration changes overestimate the total glacial/interglacial change in air concentration by up to 60% for sea salt and 130% for mineral dust. In the following we will discuss Antarctic flux records when we are interested in atmospheric aerosol concentrations over the East Antarctic plateau.

3.2. Transport

[19] As illustrated in Figures 2–7, sea salt and mineral dust show a high covariance both on glacial/interglacial and in part also on millennial timescales during the glacial. The latter is exceptionally pronounced in Greenland. In principle, there are two possible explanations for these common variations: (1) The source strength of both aerosol species reacts to climate changes in a comparable way. (2) The overall transport by intensified large-scale circulation patterns leads to a covariation of both aerosol components because of changes in transport time and/or atmospheric lifetime. On the basis of an empirical orthogonal function

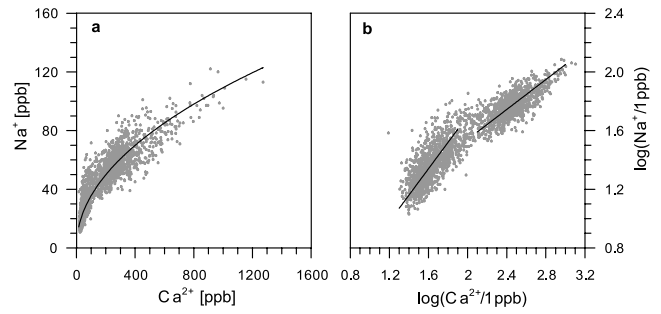


Figure 8. Scatterplot of Na⁺ and Ca²⁺ concentrations in the GISP2 ice core [*Mayewski et al., 1994, 1997*] for the time interval 25,000–50,000 years B.P. (MIS3). (a) Concentration plus a power law fit (line) over the entire data set. (b) Logarithmic concentration plus two linear regression fits (lines) as described in the text.

(EOF) analysis performed on the ion records of the GISP2 ice core, *Mayewski et al.* [1994, 1997] concluded that the high correlation of sea-salt and mineral dust ions is due to common transport of both aerosol components to Greenland. The time series of the first EOF of normalized Cl⁻, SO₄²⁻, Na⁺, K⁺, Mg²⁺, and Ca²⁺ concentrations, explaining 91% of the total variance, resembles very closely the Ca²⁺ and Na⁺ record and was termed the Polar Circulation Index (PCI) [*Mayewski et al., 1994*].

[20] However, the EOF analysis intrinsically reflects only the linear component of the covariance of each aerosol series with the principal component of EOF1 and thus only the linear component of the covariance between the different series. If Na⁺ and Ca²⁺ concentrations are compared in a scatterplot, e.g., for MIS3 (Figure 8a), where most of the variance is induced by the DO events, it is evident that such a linear relationship does not strictly hold. Instead, the coupling of both species can be better described by a power law [*Siggaard-Andersen, 2004*]. The question arises whether such a relationship can be explained by aerosol transport to the ice sheet. In a first-order approximation the change in aerosol concentration of an air parcel along its trajectory can be written as

$$C_{\text{air}}(t) = C_{\text{air}}(0)e^{-(t/\tau)}, \quad (3)$$

where t is the transport time, τ is the atmospheric aerosol lifetime, and $C_{\text{air}}(0)$ is the air concentration at the source [*Hansson, 1994*]. If we consider two aerosol species (e.g., Na⁺ and Ca²⁺), equation (3) leads to

$$C_{\text{Na}^+} = C_{\text{Na}^+}(0)C_{\text{Ca}^{2+}}^{-\alpha}(0)C_{\text{Ca}^{2+}}^{\alpha} \quad (4)$$

and in logarithmic form

$$\log C_{\text{Na}^+} = \log C_{\text{Na}^+}(0) - \alpha \log C_{\text{Ca}^{2+}}(0) + \alpha \log C_{\text{Ca}^{2+}}, \quad (5)$$

with $\alpha = \frac{t_{\text{Na}^+} + \tau_{\text{Ca}^{2+}}}{t_{\text{Ca}^{2+}} + \tau_{\text{Na}^+}}$.

From equations (4) and (5) it follows that if both species were subject to a covariant change in transport time t or in atmospheric lifetime τ (i.e., $\alpha = \text{const}$), a power law dependence of Na^+ and Ca^{2+} concentrations, implying a linear relationship in logarithmic concentrations, would be expected [Siggaard-Anderson, 2004]. Such a covariant change in t_{Na^+} and $t_{\text{Ca}^{2+}}$ could be caused by a general hemispheric intensification of transport; however, changes in long-range transport of dust from Asian desert areas to the Greenland ice sheet and meridional transport of sea salt related to cyclonic activity in the North Atlantic were uncoupled. A common scaling of τ_{Na^+} and $\tau_{\text{Ca}^{2+}}$ can be expected from an overall hemispheric reduction of precipitation, thus wet deposition along the transport routes of dust and sea salt. Again, a reduction of wet deposition in the past may not necessarily have been the same for the different transport routes of sea salt and dust. Note that a coupling of sea-salt and mineral dust aerosol by transport does not hold for individual precipitation events, because variability in transport time and aerosol scavenging for individual trajectories is very large. However, ice core aerosol records with decadal or even centennial resolution integrate over many precipitation events and efficiently average this variability out. Accordingly, ice core data are able to record changes of the average transport of aerosol to the ice sheets only.

[21] An independent change in the source strengths ($C_{\text{Na}^+}(0)$, $C_{\text{Ca}^{2+}}(0)$) of one or both species or a completely decoupled transport of dust and sea salt to the Greenland ice sheet would destroy a linear relationship in equation (5). Only if the source strengths of both species are correlated could a power law relationship also be caused by changes in emissions. For sea salt and mineral dust where the climate conditions at the sources are distinct, this appears not to be likely but cannot be excluded per se. Accordingly, the existence of a power law relationship between mineral dust and sea-salt species is expected if covariant transport changes occurred; however, a coupled source effect for sea salt and dust could also explain a high covariance. In the following we will study what potential implications equation (5) has for the interpretation of aerosol ice core records in terms of transport changes.

[22] When switching from one climate state to the other (e.g., going from the LGM to the Holocene or from stadials to interstadials), circulation patterns transporting mineral dust and sea salt to the ice sheets as well as precipitation rates leading to wet deposition en route may change and potentially lead to a change of α (in equations (4) and (5)). In that case, no clear linear coupling of logarithmic sea-salt and dust concentrations can be expected. Indeed, in the scatterplot in Figure 8b, different linear relationships, and thus different α , are observed for cold stadials and warm interstadials (here separated according to $\text{Ca}^{2+} > 100$ ppb and $\text{Ca}^{2+} < 100$ ppb, respectively) as has also been observed in scatterplots for Ca^{2+} versus isotope temperature [Fuhrer et al., 1999].

[23] Using two-dimensional linear regression analysis, the following linear fits can be derived for the individual groups in Figure 8b:

Stadials

$$\log(C_{\text{Na}^+}/1 \text{ ppb}) = 0.52 + 0.51 \log(C_{\text{Ca}^{2+}}/1 \text{ ppb}), r^2 = 0.58$$

Interstadials

$$\log(C_{\text{Na}^+}/1 \text{ ppb}) = -0.10 + 0.90 \log(C_{\text{Ca}^{2+}}/1 \text{ ppb}), r^2 = 0.52.$$

According to equation (5) these regressions imply that 50–60% of the variance in Na^+ and Ca^{2+} records could be explained by a common transport effect within stadials and interstadials, respectively. Alternatively, dust and sea-salt sources may have responded to climate changes in a similar way during both stadials and interstadials. A linear relationship can be also derived for the Holocene concentrations (not shown) with

Holocene

$$\log(C_{\text{Na}^+}/1 \text{ ppb}) = -0.12 + 0.95 \log(C_{\text{Ca}^{2+}}/1 \text{ ppb}), r^2 = 0.18.$$

Interestingly, the linear regression parameters for the Holocene are identical to the interstadial values, suggesting that atmospheric aerosol transport was not significantly different for interstadial events and the Holocene. Note, however, that the Holocene linear relation explains only 18% of the total variance during the Holocene, implying that the coupling of sea salt and dust is weak and the agreement between interstadial and Holocene slopes may be accidental.

[24] For the shift between stadial and interstadial regimes the different regression lines in Figure 8 imply that no common transport-related covariance in sea salt and mineral dust can be assumed across stadial/interstadial transitions. Accordingly, a definition of a joint PCI for both regimes has to be questioned. In contrast, a sudden switch in the power α occurred, which may be attributed to a fast switch in atmospheric transport (leading to a different change in atmospheric transport or lifetime for Ca^{2+} compared to Na^+) or a sudden change in the source strength for mineral dust and/or sea salt.

[25] Unfortunately, the coarse-resolution GISP2 ion record does not allow precise resolution of the timing of this decoupling. On the GRIP ice core, Ca^{2+} has been measured at high resolution using continuous flow analysis [Fuhrer et al., 1999], but sea-salt data are not available at similar resolution. Only recently, has the new NorthGRIP ice core [North Greenland Ice Core Project Members, 2004] been completed, where continuous CFA records have been measured for both Ca^{2+} and Na^+ at 1 cm resolution. In Figure 9 an example of the latest CFA data from the NorthGRIP ice core is shown for the time period around IS3 and IS4. A sudden shift in the slope of Ca^{2+} during the transition out of IS4 (at 1882.7 m) and into IS3 (at 1869.1 m) can be recognized. During the stadial/interstadial transition

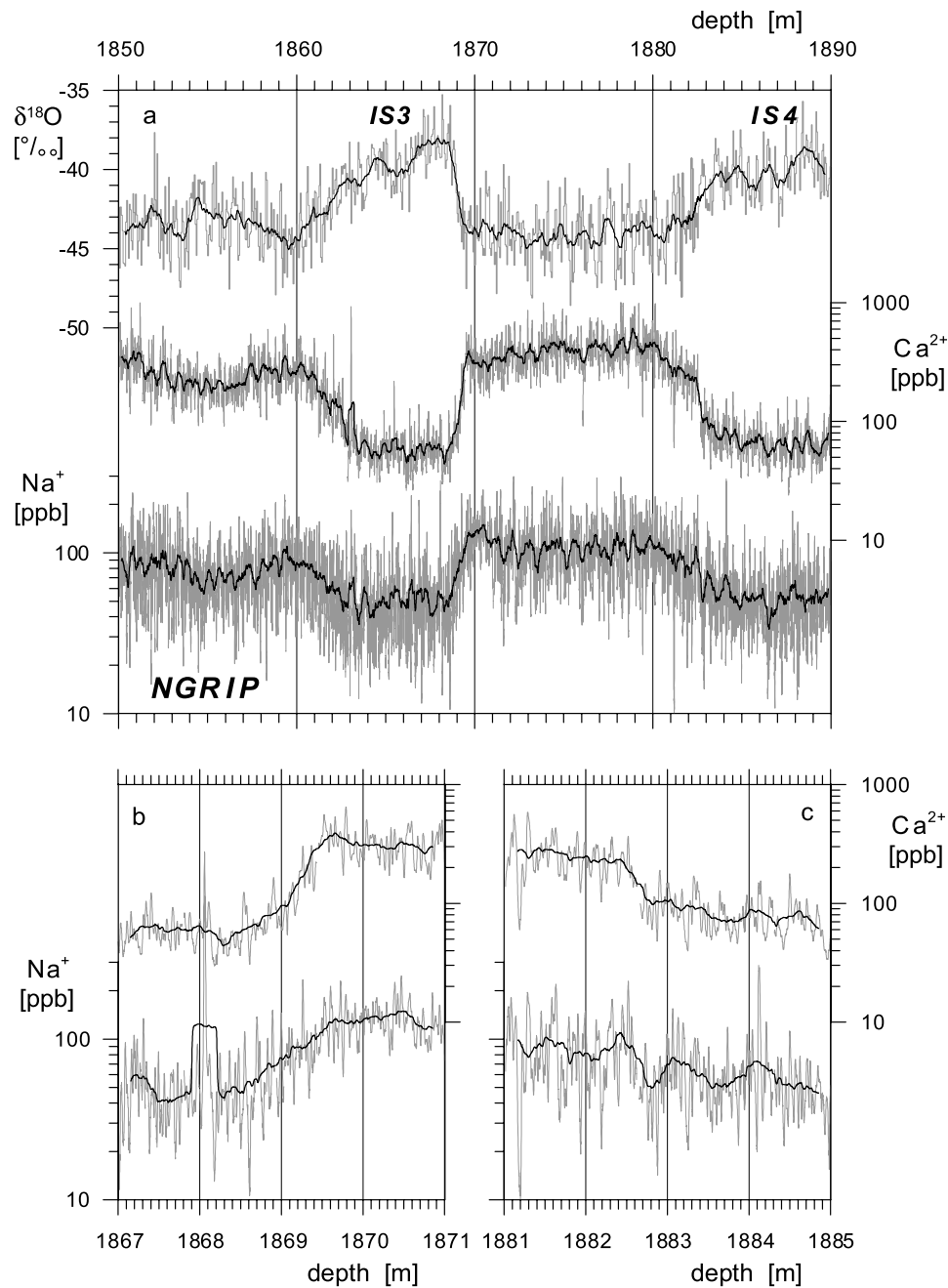


Figure 9. Example of high-resolution continuous flow analysis records in the NorthGRIP ice core: (a) overview of the time period around IS3 and IS4 for $\delta^{18}\text{O}$ (S. Johnsen, unpublished data, 2006), Na^+ and Ca^{2+} (M. Bigler, unpublished data, 2006) and details of Na^+ and Ca^{2+} records over the transition (b) into IS3 and (c) out of IS4. High-resolution data are displayed by thin shaded lines; thick black lines represent a 30-point moving average for $\delta^{18}\text{O}$ and a 300-point moving average for Na^+ and Ca^{2+} .

the decline in Ca^{2+} becomes suddenly slower, while the rate of the Na^+ increase remains the same. Vice versa dust suddenly increases from the interstadial to the stadial, while sea salt shows a more gradual increase. This is exactly what is observed in Figure 8b where the slope in the Na^+ versus Ca^{2+} scatterplot declines for cold intervals. The abruptness of this shift in Figure 9, which occurs in only a couple of years, is outstanding and points to a sudden atmospheric reorganization, which could be linked to a shortcut in the transport paths from the Chinese deserts to Greenland. Increased dust emissions by a drastically changed dust

storm frequency or dust uplift may also result from a sudden change in atmospheric circulation at the dust source. In contrast, changed weathering or soil surface conditions and vegetation cover at the source area are unlikely to change dust emissions from one year to the other [Zou and Zhai, 2004]. An extended evaluation of the high-resolution CFA data for other stadial/interstadial transitions in this respect is currently under way and will show whether this sudden shift is a persistent feature for all stadial/interstadial transitions.

[26] While the change in aerosol composition may give some indication of transport and/or source changes, it is not

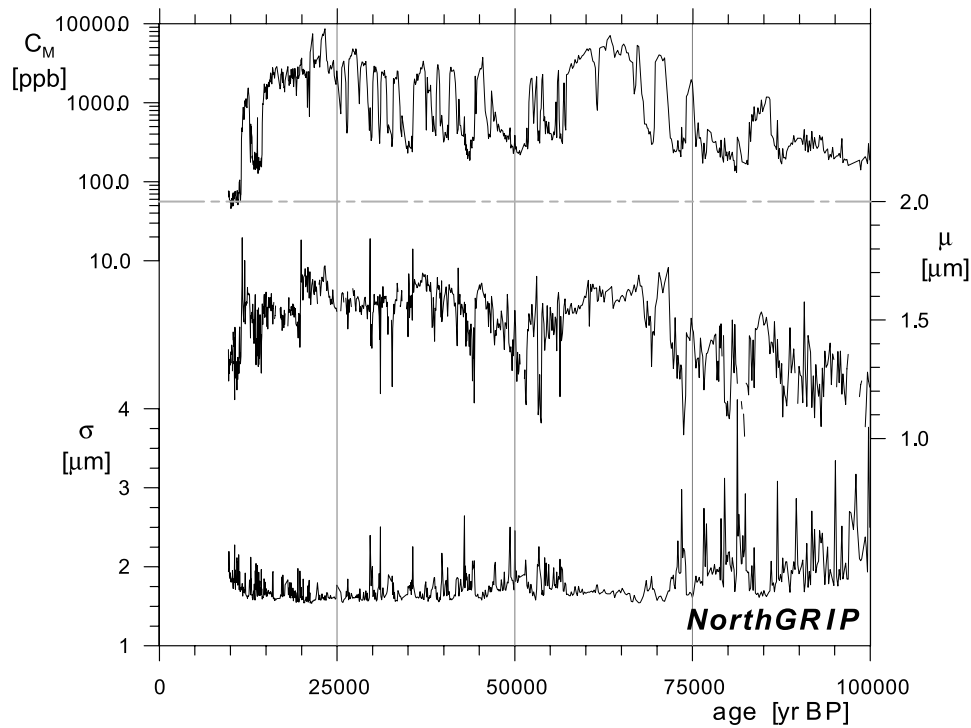


Figure 10. Continuous (1.65 m averages) profiles of the particulate mineral dust concentration and size distribution in the ice core [Ruth et al., 2003]. Shown are the mass concentration C_M , the mode μ , and the standard deviation σ of lognormal distributions fitted to the size spectra in the interval 1–7.5 μm . The dashed-dotted line indicates the Preboreal mass concentration level.

a conclusive parameter to quantify the transport effect. Fortunately, the size distribution of insoluble mineral dust, which is essentially independent of the source strength, also allows an estimation of the change in transport time t (see Appendix A) and has been measured on selected intervals of Greenland ice cores [Steffensen, 1985, 1997; Zielinski and Mershon, 1997]. Latest techniques allowed also for a continuous determination of the size distribution in the NorthGRIP ice core [Ruth et al., 2003] as shown in Figure 10. The outstanding result of these studies is that the average size mode of dust in Greenland during the LGM is 0.3–0.4 μm larger than for the Preboreal. Also, stadial dust appears to be generally about 0.2–0.4 μm larger than interstadial dust particles, although the scatter in the size mode on this timescale is considerable. Taking the results of a conceptual simplified transport model (as presented by Ruth et al. [2003] and modified in Appendix A) at face value, this translates into a reduction in transport time (comprising both changes in wind speed as well as length and spatial configuration of the transport path) of about 50% during the LGM compared to the PB. For the stadial/interstadial transitions a reduction in transport time by about 35% appears possible, dependent on the particle size taken to be representative of glacial and interstadial conditions in Figure 10.

[27] According to equation (3) we can write for the change in atmospheric aerosol concentration on top of the ice sheet

$$\frac{C_{\text{air}}^{\text{cold}}}{C_{\text{air}}^{\text{warm}}} = \frac{C_{\text{air}}^{\text{cold}}(0)}{C_{\text{air}}^{\text{warm}}(0)} \exp\left[\frac{t^{\text{warm}}}{\tau^{\text{warm}}}\left(1 - \frac{t^{\text{cold}}}{t^{\text{warm}}}\frac{\tau^{\text{warm}}}{\tau^{\text{cold}}}\right)\right]. \quad (6)$$

The exponential term on the right-hand side of equation (6) parameterizes the transport-induced change in aerosol concentration, and the scaling factor $C_{\text{air}}^{\text{cold}}(0)/C_{\text{air}}^{\text{warm}}(0)$ comprises any source changes from warm to cold climate conditions. On the basis of the outcome of the conceptual model, changes in the size distribution imply that $t^{\text{LGM}}/t^{\text{PB}} \approx 0.5$ (see also Appendix A). In order to evaluate $\tau^{\text{PB}}/\tau^{\text{LGM}}$ we consider wet and dry deposition en route, where at lower latitudes wet deposition always dominates over dry deposition. Modeling considerations by Andersen and Ditlevsen [1998] allow us to estimate that the average precipitation rate in the LGM A^{LGM} was about 50% of that in the Preboreal period A^{PB} , and thus $\tau^{\text{PB}}/\tau^{\text{LGM}} \approx 0.5$. The ratio between transport time and lifetime for the PB can be estimated from recent trajectory studies, where t is on the order of 10 days for the transport of dust from east Asia to Greenland [Kahl et al., 1997]. The atmospheric lifetime of particulate dust has been estimated in atmospheric circulation model studies to be about 4–10 days [Mahowald et al., 1999; Tegen and Fung, 1994; Timmreck and Schulz, 2004; Werner et al., 2002]. Accordingly, $t^{\text{PB}}/\tau^{\text{PB}}$ is somewhere between 2.5 and 1. We take $t^{\text{PB}}/\tau^{\text{PB}} = 2$ as a best guess. Accordingly, a transport-induced change in atmospheric dust concentrations by a factor of 4.5 (with a range from 2 to 12) is possible according to these one-dimensional model considerations without invoking any additional change in $C(0)$ in equation (6).

[28] For interstadial periods, no information on aerosol life time is available from atmospheric general circulation model (GCM) experiments. We estimate the accompanying

precipitation change as only 50% of that from the LGM to the Preboreal ($\tau^{IS}/\tau^S = 0.75$), use the transport time derived from the size distribution of $t^S/t^{IS} = 0.65$ (see Appendix A), and estimate $t^{IS}/\tau^{IS} = 2$ as for the Preboreal. With these assumptions we arrive at a transport-induced change in aerosol concentration from interstadials to stadials of a factor of 3 (with a range of 2–5, dependent on the value taken to be representative for the mode during interstadials).

[29] These numbers compare to an observed increase in dust concentration of a factor of 80 for LGM/Holocene and a factor of 15 for stadial/interstadial transitions, which only slightly overestimate the change in atmospheric concentration (see section 3.1). In conclusion, the change in transport and lifetime is an important process for long-term changes in atmospheric dust, but it can explain only 15% of the glacial/interglacial and 40% of the observed stadial/interstadial concentration changes, implying that significant changes in the dust source areas (such as aridity or local wind speeds) must have also occurred [Ruth et al., 2003]. A similar conclusion has also been drawn in an earlier study [Fuhrer et al., 1999] based solely on concentration records and conceptual model considerations. Given that the effect in Figure 8 is solely due to transport, we can apply the change of transport time for dust at face value to sea-salt aerosol and use the scaling factor α as determined from the slopes in Figure 8. This scaling factor α is smaller during stadials, which implies that the change in transport time for mineral dust was larger than for sea salt during stadials. Accordingly, the factor for the rise of sea-salt concentrations due to transport changes during interstadial/stadial transitions was most likely smaller than the dust-derived factor of 3.

[30] For Antarctica a common influence of transport efficiency on sea-salt and mineral dust aerosol seems to be even less important than for Greenland. As outlined in Figures 3, 4, and 7 the sensitivity of changes in sea-salt aerosol to climate variations is significantly smaller than for mineral dust. This is also illustrated in the scatterplot shown in Figure 11. Here we used fluxes instead of concentrations, because fluxes are more representative of atmospheric concentrations in the low-accumulation areas of the East Antarctic plateau, and corrected for the sea-salt and crustal contribution in Ca^{2+} and Na^+ , respectively (note, however, that the picture looks essentially the same for concentrations). Two clouds of points emerge for cold glacial and warm Holocene conditions. However, in contrast to Greenland, mineral dust is essentially uncorrelated to sea salt in the Holocene as reflected in the large range of sea-salt fluxes compared to constantly low fluxes of mineral dust. Vice versa in the glacial period, sea-salt fluxes exhibit rather constant values of around $80 \text{ ng cm}^{-2} \text{ yr}^{-1}$ while the mineral dust flux is highly variable at that time. Accordingly, there seems to be no strong functional dependence between sea salt and mineral dust [Röthlisberger et al., 2002], and a common change in transport time or atmospheric lifetime is unlikely to dominate the sea-salt and dust variations within either the Holocene or the glacial. Note, however, that transport paths of both species to Antarctica are different and may have experienced unrelated changes.

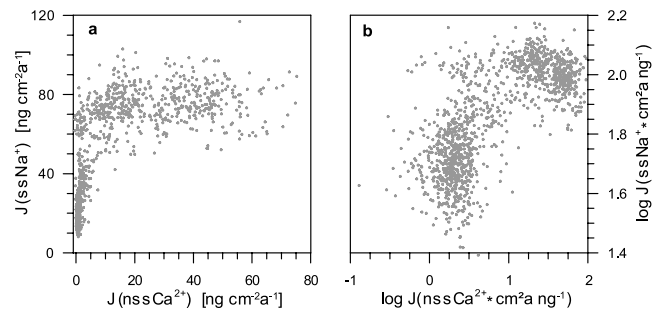


Figure 11. Scatterplot of sea-salt and mineral dust fluxes in the EDC ice core [Röthlisberger et al., 2002] over the last 45,000 years: (a) ssNa^+ versus nssCa^{2+} fluxes and (b) logarithmic fluxes for ssNa^+ versus nssCa^{2+} .

[31] Because of the extremely low accumulation rates on the East Antarctic plateau, no seasonally resolved records for sea salt and mineral dust have been obtained that would allow us to further disentangle source and transport changes. However, size distribution measurements have been performed on central Antarctic ice cores [Delmonte et al., 2002, 2004b; Petit et al., 1990], which may help to quantify the transport effect by observations. Unfortunately, the outcome of these studies is ambiguous. While size distributions at Dome C and also at Komsomolskaya (located about 900 km west of Dome C and 550 km north of Vostok) support a $0.2\text{--}0.4 \mu\text{m}$ smaller mode of the size distribution at the LGM compared to the early Holocene, the same parameter at Dome B (located closer to Vostok) shows the opposite behavior, i.e., significantly ($0.4\text{--}0.5 \mu\text{m}$) larger particles in the late glacial [Delmonte et al., 2004b]. This would imply a longer glacial transport time and thus a reduction in atmospheric dust concentrations at Dome C but a shorter transport time for Dome B! Delmonte et al. [2004b] argue that two different pathways must exist for dust in Antarctica. They suggest that smaller particles could be delivered preferentially by upper tropospheric transport, while larger particles may be transported along a lower-altitude pathway. Accordingly, Delmonte et al. [2004b] interpret small particles as being associated with the center of atmospheric subsidence in the polar vortex. Thus, if this hypothesis is correct, the ice core results would point to a stronger subsidence of high-altitude air masses at Dome C and Komsomolskaya in the glacial than during the Holocene, while Dome B shows the opposite behavior. At first glance this hypothesis is in contradiction with the higher altitude of Dome B (3650 m above sea level (asl)) compared to Dome C (3233 m asl) and Komsomolskaya (3500 m asl) and its greater distance from the coast. Preliminary dust size measurements on the new EPICA ice core in Dronning Maud Land located in the Atlantic sector of Antarctica show, on average, similar particle sizes during the Holocene and the LGM; however, individual large-particle events occur mainly during the Holocene, with vigorous transport on the ice sheet at those times. In summary, the opposite behavior of particle size changes for

different ice cores underlines the complexity of transport processes to the ice sheet and precludes a generalized estimate of the change in transport efficiency to Antarctica.

3.3. Changes in Sources

[32] While hemispheric transport of sea salt and mineral dust to remote areas is linked to overall changes in atmospheric circulation and the deposition of both species on top of the ice sheets follows similar processes, the sources of these two aerosol species are geographically distinct, and aerosol generation over the ocean and continental desert regions may be linked to different synoptic weather patterns.

3.3.1. Mineral Dust

[33] Mineral dust aerosol formation is most efficient in arid and potentially semiarid regions, where weathering is sufficiently high to replenish fine dust particles, while soil moisture is sufficiently low to allow for dust mobilization. In contrast, hyperarid regions, such as the core of the Australian continent, are most often depleted in available dust because weathering rates are too small and deflation has been active for a long time period [Rea, 1994]. In the source regions, dust mobilization is dependent on surface wind speed u , causing dust fluxes into the atmosphere to be proportional to u^3 whenever the wind speed exceeds a threshold velocity, which is soil-moisture-dependent [Gillette and Passi, 1988; Gillette et al., 1980; Marticorena and Bergametti, 1995].

[34] Since the advent of satellite imagery a global picture of modern dust emissions and long-range export of mobilized dust plumes has been obtained. Recently, Prospero et al. [2002] published an overview of active dust sources based on an aerosol absorption index derived from the Total Ozone Mapping Spectrometer. This identified the North African and Arabian peninsula desert regions as the main source for dust globally with significant westward transport of dust over the subtropical Atlantic. However, arid areas in Asia and here especially the desert regions in China (Tarim Basin, Taklamakan, and Gobi Desert) also represent efficient dust sources leading to long-range transport of dust over the Northern Pacific [Gong et al., 2003; Prospero et al., 2002]. Although overall dust emissions in the Southern Hemisphere are much smaller than in the north, important modern dust sources are located in Australia, in some regions of southern Africa, and in South America (Bolivian Altiplano and Patagonia). For glacial times most of these sources were also active, as reflected in loess formations as well as increased deposition of eolian dust in the pelagic ocean downwind of these sources (see Kohfeld and Harrison [2001], Porter and An [1995], Rea [1994], Sun [2002], Xiao and An [1999], and their references).

[35] Ice core studies provide important clues for the identification of source regions of dust. Studying the mineralogical composition of dust in the GRIP ice core, Maggi [1997] has shown that dust generation during warm periods was dominated by chemical weathering, while during cold periods physical weathering became more important. Isotopic provenance studies represent an even more powerful tool to constrain source regions. For Greenland the Sr/

Nd isotopic composition clearly points to Asian desert regions in China as the primary source for dust today and in glacial times [Biscaye et al., 1997; Bory et al., 2003; Svensson et al., 2000]. These provenance studies, however, are only as unambiguous as reference samples of dust from desert regions exist. This represents a particular problem if new dust source regions were activated during the glacial, as, e.g., exposed shelf areas or high-latitude Arctic regions, for which no modern reference samples are available. The isotopic provenance studies are also in line with recent trajectory studies of air mass transport to Greenland [Kahl et al., 1997], which show that the majority of trajectories enter Greenland from the west, virtually excluding the Sahara as an important dust source for the Greenland Ice Sheet.

[36] In Antarctica, comparable isotopic studies have been performed [Basile et al., 1997; Delmonte et al., 2004a, 2004b; Grousset et al., 1992]. Again, the problem of the availability of reference samples for all possible source areas applies. Despite this limitation these studies clearly show that the dust deposited during the glacial at all the investigated ice core drill sites in East Antarctica is derived mainly from Patagonia with substantial contributions also from Australia [Revel-Rolland et al., 2006] during the Holocene. A shift in terrestrial dust composition is also suggested by a change in the $^3\text{He}/^4\text{He}$ ratio in particulate terrestrial dust as derived from the EPICA ice core in Dronning Maud Land [Winckler and Fischer, 2006]. A strong Patagonian source is also broadly in line with air trajectory studies [Reijmer and van den Broeke, 2000; Reijmer et al., 2002], which show that air mass transport to all Antarctic ice core drill sites follows a cyclonically curved pathway, which originates in the low-pressure trough around the Antarctic continent. Only Patagonian dust sources seem to be high enough in latitude to fuel those circulation patterns with mineral dust. A similar trajectory study by Lunt and Valdes [2001] based on atmospheric GCM results forced with modern and LGM sea surface temperatures (SSTs) also supports a predominant South American origin of aeolian dust in Antarctica both today and at the LGM.

[37] The question remains whether exposed Argentine Shelf areas may have added to the Patagonian dust sources during the glacial. On the basis of Al, Ca, and Mg measurements over the last glacial cycle in the Vostok ice core, de Angelis et al. [1992] conclude that glacial dust originated in part from marine carbonates. de Angelis et al. [1992] estimates that up to 50% of the dust during the glacial may originate from exposed continental shelf areas. However, the identification of mineralogy based on bulk concentrations in ice core samples is not unambiguous. Measurements of the Sr/Nd isotopic composition by Basile et al. [1997] yielded a small difference between ice core and marine reference samples from the Argentinean Shelf. However, this offset is now explained as the result of different size fractions showing different isotopic compositions, and the Argentine Shelf cannot be excluded on the basis of these measurements [Delmonte et al., 2007]. Independent information on the role of Argentine shelf

areas as sources for Antarctic dust can be derived from a comparison of the temporal evolution of glacial/interglacial sea level changes and dust fluxes in Antarctica. For older terminations the relative dating uncertainty of sea level estimates and ice core dust records does not allow an unambiguous answer. During the last termination, however, major shifts in sea level on the Argentine shelf [Gulderson et al., 2000] significantly lagged the strong decline in dust at the beginning of the transition [Wolff et al., 2006]. In contrast to the late global ice volume decline, hence sea level increase, an early Patagonian deglaciation is supported by some geomorphological evidence [Sugden et al., 2005]. In summary, a dominant increase in the continental dust source in Patagonia appears to be more likely to explain the Antarctic dust variations than exposed shelf areas.

3.3.2. Sea-Salt Aerosol

[38] Although sea salt represents the most abundant aerosol component in the atmosphere, considerably less is known about the sources of sea-salt aerosol for the Greenland and Antarctic ice sheets. One reason is the lack of isotopic tracers to constrain the geographical origin of sea-salt aerosol because the ocean is well mixed. In particular, the influence of sea-salt aerosol derived from sea ice versus that derived from the open ocean on the sea-salt budget on the ice sheets is still an open question. Globally, the most important source of sea salt is the dispersion of seawater over the open ocean, which is also dependent on wind speed. Different parameterizations exist, approximating the wind speed dependence of the sea-salt generation flux by a power or exponential law [Guelle et al., 2001]. Highest wind speeds and efficient transport of sea-salt aerosol to the polar ice sheets are connected to cyclonic activity over the open ocean, which is concentrated along the polar fronts in both hemispheres. Accordingly, ice core chemistry [Fischer and Mieding, 2005; Fischer et al., 2004; Kreutz et al., 2000] and meteorological [Chen et al., 1997; Noone et al., 1999; Reijmer and van den Broeke, 2000; Simmonds and Keay, 2000] studies were able to show that recent sea-salt deposition and precipitation both in Greenland and Antarctica are closely connected to cyclonic activity over the North Atlantic and the Southern Ocean, respectively. This effect comprises both efficient generation and uplift of sea salt within frontal systems as well as the guidance of storm tracks by large-scale pressure patterns onto the ice sheets. A recent study by Fischer and Mieding [2005] revealed a doubling of multidecadal Na^+ concentrations in northern Greenland in parallel to SST variations of approximately 0.5°C over the last 150 years. Periods of higher sea-salt concentrations have been related to changes in storm tracks over the North Atlantic in this study. Applying this modern relationship to the glacial, the sea salt increases during Dansgaard-Oeschger events would require a surface cooling of about 2°C , which is at the lower end of values observed in marine sediment records [McManus et al., 1999]. Of course, this late Holocene relationship cannot be directly extrapolated to glacial conditions when sea ice coverage and storm tracks had considerably changed. However, it shows that changes in storm tracks even during rather stable warm climate conditions can result in large

effects on sea-salt aerosol deposition on the Greenland ice sheet.

[39] Dispersion of frost flowers, generated on the water surface during the formation of sea ice, has recently been reported to represent another efficient way to produce sea-salt aerosol (hereinafter referred to as sea ice salt) especially for coastal regions close to the sea ice formation zone [Rankin et al., 2000; Rankin and Wolff, 2003; Wagenbach et al., 1998]. This process may also represent a potential sea-salt aerosol source for the Antarctic plateau [Wolff et al., 2003]. During this process the precipitation of mirabilite ($\text{Na}_2\text{SO}_4 \cdot 10\text{H}_2\text{O}$) leads to a weak depletion of Na^+ and a strong depletion of SO_4^{2-} relative to Cl^- in frost flower derived-sea-salt aerosol particles relative to ocean water. This effect can be clearly discerned in coastal Antarctic aerosol samples [Wagenbach et al., 1998]. A detection of sea ice salt in the interior of the ice sheet using its characteristic ionic composition, however, is difficult. Among other reasons this is because Cl^- in Antarctic aerosol and snow [Röthlisberger et al., 2003; Wagenbach et al., 1998] often shows an enrichment compared to Na^+ in summer because of a larger atmospheric lifetime of gaseous HCl released from sea-salt aerosol in acidic environments [Legrand et al., 2002; Legrand and Delmas, 1988]. In addition, the dominance of other SO_4^{2-} sources in the sulfate budget on the ice sheets in summer and partly in winter [Fischer et al., 1998b; Hammer et al., 1997; Legrand, 1995] masks a sea ice salt contribution for both recent as well as glacial conditions. However, some aerosol evidence exists: One selected sea-salt aerosol deposition event at South Pole station showed a clear sulfate depletion [Wolff et al., 2003]. In addition, 1 year of aerosol sampling at Dome Fuji on the East Antarctic plateau revealed unambiguous evidence of sulfate-depleted sea-salt aerosol during austral winter [Hara et al., 2004] with the degree of the sulfate depletion being similar to coastal Antarctic sites. On the basis of air mass trajectories originating in the midlatitudes, Hara et al. [2004] discarded a sea ice origin of those fractionated sea-salt events at Dome Fuji and suggested a local fractionation process by evaporation at the snow surface. However, postdepositional changes in the snowpack have never been observed for Na^+ or SO_4^{2-} . In addition, the air mass trajectories to Dome Fuji [Hara et al., 2004] passed over the sea ice zone and may have picked up fractionated sea ice salt en route. In summary, we feel that the aerosol samples from Dome Fuji represent the so far strongest direct evidence documenting an influence of sea ice salt formation on the sea-salt aerosol budget of the interior of Antarctica. However, a quantitative estimate of the relative contributions of sea-salt aerosol from the open ocean and from sea ice has not been established yet for the East Antarctic plateau.

[40] What circumstantial evidence does exist for a recent contribution of frost flowers to the sea-salt deposition on the Antarctic plateau? The seasonal variation of sea-salt species in ice cores shows a maximum in winter/spring in Dronning Maud Land, where snow accumulation is high enough to resolve annual cycles [Göktas et al., 2002; Sommer et al., 2000]. This is the time when sea ice is at its maximum, and

therefore the open water source is located farthest away. Frost flower formation occurs whenever surface temperatures are cold enough to sustain refreezing of wind driven leads, which may occur everywhere in sea ice-covered areas. To first order the sea ice salt source is therefore expected to be proportional to the areal extent of winter sea ice cover for modern conditions. However, the transport time of sea ice salt aerosol to the central Antarctic increases the farther away sea ice salt is formed. Accordingly, the influence of a sea ice salt source diminishes with distance to the drill site. On the other hand, transport velocities are increased in winter for modern conditions [Reijmer et al., 2002], compensating at least partly for the increased distance of a sea ice and open ocean aerosol source. In addition, summer sea ice may also represent a sea ice salt source if temperatures are low enough to sustain refreezing of leads as may have been partly the case during the glacial.

[41] On the basis of this observational evidence for sea ice salt formation in ice-covered areas we attempt to estimate the potential increase of this source during the glacial. If we assume that the amount of freshly formed sea ice in open leads (thus of potentially frost flower-covered regions) is proportional to the sea ice coverage and neglect the effect of transport distance, we can estimate a maximum increase in the source of sea ice salt for the glacial using paleoreconstructions of sea ice extent. We estimate that the modern winter sea ice edge is located on average at around 60°S around Antarctica. Reconstructions of the sea ice extent in the glacial point to a substantially larger sea ice extent in winter reaching as far as 45°S and beyond. On average we use a value of 50°S for the glacial winter sea ice edge [Cooke and Hays, 1982; Crosta et al., 1998; Gersonde et al., 2003, 2005]. Today the summer sea ice edge is close to the coast in most areas of the Antarctic continent or to the edge of the offshore ice shelves (approximately 70°S). During the glacial the summer sea ice extent was increased to about 60°S in some regions such as the Weddell Sea, while in others it was unchanged, although the summer sea ice evidence is scarce. For our estimate this may imply a considerable amount of perennial sea ice, which may not be as efficient as a sea ice salt source. Accordingly, we calculate an upper limit of the sea ice salt source by assuming that perennial and seasonally covered areas contributed equally to the sea ice salt source. In that case we add the area of summer sea ice cover to the winter area to calculate a total sea ice area. This area is compared to the recent winter sea ice coverage, which is the only season contributing to sea ice salt formation today. In addition, we calculate a lower limit where we assume that perennial sea ice did not contribute to sea ice salt formation at all, which probably underestimates the real conditions. Using these assumptions, the sea ice salt source may have been between 1.6 and 3.2 times more extensive during the glacial. This does not necessarily imply that the sea ice salt formation was also a factor of 2–3 larger in the LGM than in the Holocene, because areas covered by sea ice in the glacial but not in the Holocene are open ocean sources for sea-salt aerosol in the Holocene. So far the lack of any systematic

flux studies on the sea ice salt formation process precludes a better quantification.

[42] For Greenland the situation is even more complex. Sea ice in the modern North Atlantic is mostly formed in the Arctic basin and exported through Fram and Davis straits and melts slowly when entering warmer waters. In situ formation of sea ice is therefore only of secondary importance in the North Atlantic. Thus there are only limited regions of active sea ice salt formation around central and southern Greenland today. We conclude that the open ocean is the primary sea-salt source for modern conditions, and cyclonic activity over the northern Atlantic leads to transport of sea-salt aerosol onto the Greenland ice sheet.

[43] For the LGM, cyclonic activity was still strong over the Atlantic, and a permanent cyclone has been found in an atmospheric GCM over Baffin Bay [Krinner and Genthon, 1998]. However, sea ice extent was also greatly enhanced in the North Atlantic at that time. To answer the question of the potential role of sea ice salt for the sea-salt deposition on top of the Greenland ice sheet during the LGM, reconstructions of sea ice extent become crucial. In the recent Glacial Atlantic Ocean Mapping (GLAMAP) 2000 project a renewed effort was made to estimate SST in the North Atlantic during the LGM using foraminiferal assemblages. From this temperature information, winter and summer sea ice extents have been deduced [Pflaumann et al., 2003; Sarthein et al., 2003]. This analysis shows that the summer sea ice edge protruded to 70°–75°N and the winter ice edge extended to 50°–70°N. This is less than estimated earlier [CLIMAP Project Members, 1976, 1981] but would still imply a considerable change in sea ice extent compared to the present. The sea ice extent was derived using an empirical modern temperature calibration, which assumes the presence of summer sea ice whenever the reconstructed summer sea surface temperature was below +2.5°C and winter sea ice when winter sea surface temperatures were below +0.75° or +0.4°C. In any case these threshold temperatures are too warm to allow for in situ sea ice formation and reflect the fact that sea ice found in the North Atlantic today is mainly exported from its cold source areas in the Arctic basin into warmer North Atlantic waters. Accordingly, while this calibration may allow us to estimate the total sea ice coverage for the LGM it does not allow us to quantify the area of in situ sea ice formation. While cold temperatures and katabatic winds along the east coast of Greenland may have allowed for glacial in situ sea ice formation, the total area of potential frost flower formation was clearly smaller than the ice cover estimated by GLAMAP2000. This reduces the importance of an increased glacial North Atlantic sea ice salt source to the sea-salt aerosol budget for the Greenland ice sheet significantly.

4. AEROSOL GENERATION AND TRANSPORT IN GENERAL CIRCULATION MODELS

4.1. Modeled Changes in Aerosol Emissions

[44] Various modeling studies have been performed to simulate changes in dust emissions in potential source

regions and to compare them to dust records from polar ice sheets for glacial and interglacial conditions. First attempts failed to simulate significant glacial increases in ice core concentrations [Genthon, 1992; Joussaume, 1990, 1993]. However, more recent models were able to simulate considerable increases in the source strength of mineral dust. In general, an intensification of global dust emissions of a factor of 2–3 can be derived from those models; however, the reasons for these increases differ considerably between different modeling studies, with changes in wind speed [Reader et al., 1999; Werner et al., 2002], soil moisture [Andersen et al., 1998; Reader et al., 1999], and/or vegetation cover [Mahowald et al., 1999; Werner et al., 2002] contributing to the simulated changes. Emission changes for Asian deserts and Patagonia, which are most relevant for dust changes in Greenland and Antarctica, respectively, also changed by a factor of 2–3 in these models. An underestimation of dust emissions from central Asia for modern conditions is indicated by dust deposition which is a factor of 5 too low close to the Asian source [Mahowald et al., 1999]. Again, modern dust deposition on the Greenland ice sheet is a factor of 2–5 too high in some modeling studies [Andersen et al., 1998; Mahowald et al., 1999], probably related to an overestimation of transport of background dust aerosol from lower latitudes.

[45] In the models by Mahowald et al. [1999] and Werner et al. [2002], which include an interactive vegetation scheme, the expansion of existing dust sources and the activation of additional high-latitude dust source regions (Siberia, Kamchatka, and Alaska) during the glacial play a significant role. Mahowald et al. [1999] simulated a twofold expansion of desert areas in the LGM, which led to higher global dust emissions by a factor of 3 and about 20 times higher dust loads in the northern high-latitude atmosphere. However, in the study by Werner et al. [2002], only 35% of the increase in dust emissions is caused by expansion of dust sources, while 65% (in Asia 88%) is due to an increase in wind speed. Interestingly, the total glacial dust emission in this study (about 2400 Mt yr⁻¹) is lower than the present-day emission given by Mahowald et al. [1999] (about 3000 Mt yr⁻¹). Note also that a strong contribution of high-latitude dust sources for the LGM is apparently in contradiction with the isotopic provenance studies described in section 3.3, which, however, are based on the currently limited knowledge in terms of dust provenance samples.

[46] For Antarctica a 100% glacial increase in Patagonian dust emissions and a 60% increase of Southern Hemisphere low-latitude sources compared to present day has been modeled [Andersen et al., 1998] leading to an increase in dust deposition in the Antarctic ice sheet of a factor of 1.4. Models with interactive vegetation schemes [Mahowald et al., 1999; Werner et al., 2002] predict that the majority of dust deposited in Antarctica originates from Patagonia, but significant dust deposition in Antarctica from Australian sources is found as well. Interestingly, all models overestimate recent dust deposition in Greenland but strongly underestimate it in Antarctica. The latter is so pronounced as to preclude any quantitative conclusions on changes in

the dust cycle in the Southern Hemisphere so far [Mahowald et al., 1999; Werner et al., 2002].

[47] In summary, east Asian and Patagonian dust sources have been unambiguously recognized in climate models as the main source regions for glacial age and modern dust in Greenland and Antarctica, respectively. Model studies are able to simulate an increase in dust emissions by a factor of 2–3 during the LGM. The different ways different models arrive at similar results shows that so far no consensus on the reason for dust emission changes has been reached. An underrepresentation of the Asian dust sources suggests that the meteorological situation leading to dust mobilization in this region (frontal systems and strong uplift due to topography [Sun, 2002]) is not well represented, most likely because of the insufficient spatial and temporal resolution of the models. While the limited spatial resolution suppresses important processes linked to surface topography such as uplift in mountainous regions, both spatial and temporal resolution limit the wind speed distribution. Especially the upper end of the wind speed distribution has a strong effect on dust mobilization, and an increase in gustiness during the glacial may explain another factor of 2–4 increase in dust mobilization.

[48] For sea-salt aerosol, significantly less is known from general circulation models. Most model studies take only sea-salt formation at the open ocean surface into account, while sea ice salt aerosol formation on sea ice-covered areas has only been treated in one model study [Reader and McFarlane, 2003], using a simplified emission scheme for sea ice salt generation. Those models that do not include a sea ice salt source [Genthon, 1992; Reader and McFarlane, 2003] show that the LGM sea-salt deposition in Antarctica is reduced compared to modern conditions, essentially reflecting the longer transport time from the open ocean to the ice sheet because of the expansion of sea ice. Accordingly, an enhanced glacial sea ice salt source provides an efficient means to overcome the discrepancy between expanded sea ice cover, hence larger distance to the open ocean, and increased sea-salt fluxes in Antarctic ice cores [Wolff et al., 2003]. By including a sea ice salt source, Reader and McFarlane [2003] were just able to model approximately unchanged LGM concentrations in central Antarctica compared to modern conditions; however, the strength of the sea ice salt source in that model is insufficiently constrained because of the lack of empirical flux measurements.

[49] For Greenland the model by Reader and McFarlane [2003] predicted 2.5–5 times higher sea-salt aerosol concentrations during the LGM when the sea ice salt source was included. However, in this model, sea ice coverage and hence sea ice salt formation were prescribed according to Climate: Long-Range Investigation, Mapping, and Prediction (CLIMAP) [CLIMAP Project Members, 1981], which overestimates the sea ice salt source for two reasons: first, because the CLIMAP sea ice reconstruction is now believed to overestimate sea ice coverage in the glacial North Atlantic [Pflaumann et al., 2003; Sarnthein et al., 2003] and, second, because in situ formation and export of sea ice

from the Arctic basin has not been distinguished. Clearly, more advanced modeling studies of sea ice formation in the glacial North Atlantic including sea ice salt generation are necessary to further constrain the sea ice salt source for the Greenland ice core concentrations.

4.2. Atmospheric Circulation Changes

[50] Independent information on atmospheric circulation and hence also aerosol transport changes between the LGM and the Holocene can be derived from general circulation models. In principle, a more vigorous atmospheric circulation can be expected from the larger temperature gradient between the poles and the equator during LGM conditions. Whether this leads to increased transport of aerosol to Greenland and Antarctica, however, depends on the spatial configuration of SSTs, which force glacial/interglacial changes in the strength and spatial patterns of atmospheric circulation. For example, stronger westerlies and higher cyclonic activity are modeled in northern middle latitudes [Bush and Philander, 1999; Shin et al., 2003] during the LGM; however, the core of the westerly jet is displaced by about 3° equatorward in an ocean-atmosphere GCM [Bush and Philander, 1999] as well as in simplified models [Andersen and Ditlevsen, 1998; Chylek et al., 2001; Ganopolski et al., 1998]. In addition, this overall change is modified in the Northern Hemisphere by the presence of the large ice sheets. The Laurentide Ice Sheet in particular represents a topographic barrier for atmospheric flow in the models. Accordingly, a split of the atmospheric jet into routes south and north of the Laurentide ice sheet is found in some climate models [Bromwich et al., 2004; Bush and Philander, 1999; Shin et al., 2003] for the LGM. If this split occurred, the northern branch of the jet would represent a shortened transport pathway of mineral dust from the Chinese desert regions to the Greenland ice sheet. However, the existence of a split jet stream in models is sensitive to the reconstructed altitude of the ice sheet [Peltier, 1994; Zweck and Huybrechts, 2005], which has been questioned, e.g., for Greenland [Cuffey and Clow, 1997; Raynaud et al., 1997].

[51] In the Southern Hemisphere the study by Shin et al. [2003] points to a slightly stronger zonal wind stress in the Southern Ocean for the LGM and a slight southward shift of the maximum wind stress. Despite the increased glacial wind speed in the Antarctic Circumpolar Current (ACC) region, Krinner and Genthon [1998] report a significant reduction of cyclonic activity and, on average, higher sea level pressure around Antarctica, which implies a reduced intrusion of marine air masses onto the ice sheet. For Dome C a model study by Lunt and Valdes [2001] indicates a reduced frequency of back trajectories originating over Patagonia and other continental areas in the Southern Hemisphere for the LGM, implying a reduced meridional transport of mineral dust to this site.

4.3. Modeled Changes in Aerosol Lifetime and Transport

[52] Changes in transport efficiency and atmospheric lifetime of aerosols may, in principle, be derived from those atmospheric GCMs which explicitly simulate atmospheric

transport of dust and sea-salt aerosol. Unfortunately, simulated changes in wind speed for other climate conditions also affect aerosol emissions, which, dependent on the setup of model experiments, often preclude an unambiguous separation of source and transport effects in the literature.

[53] Overall, the change in transport time in circulation models is significantly smaller than indicated by the aerosol size distribution in ice cores. In a model experiment by Tegen and Rind [2000] the latitudinal temperature gradient was increased to simulate glacial conditions while keeping the average global temperature constant. This increases the baroclinicity of the atmosphere while keeping total precipitation essentially constant. This experiment shows an increase of dust concentrations in Greenland derived from Asian dust sources by a factor 2.4. Given that the strength of the Chinese dust source in this model experiment also increased by a factor of 3.5, intensification of transport is limited in this model. In a second experiment, Tegen and Rind [2000] also reduced the global temperature, which leads to less precipitation and thus longer lifetimes of dust in the atmosphere. Doing this, the atmospheric concentration over Greenland was enhanced by an additional factor of 1.3 compared to the first experiment and by a factor of 3 compared to the modern control run. Given that the glacial increase in dust emission from Chinese dust sources was only 40% in this reduced-temperature run compared to the first experiment, an increase of Greenland concentrations by a factor of 2–3 because of a longer atmospheric lifetime can be deduced.

[54] In a two-dimensional model an increase in dust of a factor of 2–3 was deduced for Antarctica by reducing the washout rate [Yung et al., 1996] in the atmosphere. However, in more complex three-dimensional models [e.g., Mahowald et al., 1999] the global average atmospheric lifetime of dust (about 4 days) has been reported to have changed insignificantly. In a similar modeling study by Werner et al. [2002] the global average lifetime is 2.8 days today and increases to 3.5 days for the LGM, which is only a factor of 1.25. However, dust lifetimes in high latitudes have not been given explicitly. In the study by Reader et al. [1999] the change in Greenland and Antarctic concentrations due to transport and deposition en route has been specified for individual source regions. Here especially, the transport effect of dust export to Greenland from Asian sources (including a reduction in transport time and an increase in atmospheric lifetime) explains a concentration increase of a factor of 2–4, while for Antarctica a decrease in transport efficiency of 30% was deduced. In summary, while a doubling of the atmospheric lifetime by reduced precipitation rates en route [Yung et al., 1996] appears to be a sufficient way to increase atmospheric aerosol concentrations in Antarctica, the available three-dimensional model results to date do not support such a strong change.

5. SUMMARY AND CONCLUSIONS

[55] Sea-salt and mineral dust concentrations and fluxes in polar ice cores from both hemispheres are subject to

TABLE 2. Summary of the Ratios in Aerosol Source Strength, Transport/Atmospheric Lifetime, and Deposition for Mineral Dust and Sea-Salt Parameters Between the LGM and the Holocene as Well as Between Stadial and Interstadial Periods^a

Period and Parameter	Source	Transport	Deposition	Total	Observations		Additional Factor
					Concentration	Flux	
<i>Greenland</i>							
LGM/Holocene							
Dust	2.5	4.5 (2–12)	0.8	~11 (5–30)	80		7 (16–2.5)
Sea salt	2	3 (1–8)	0.8	~5 (2–13)	12		2 (6–1)
S/IS							
Dust	2.5	3 (2–5)	0.8	~6 (4–10)	15		2.5 (4–1.5)
Sea salt	2	2 (1–3)	0.8	~4 (2–6)	4		1 (2–0.7)
<i>Antarctica</i>							
LGM/Holocene							
Dust	2–3	1.3 (1–2)	1	~3 (2–4)		12	4 (3–6)
Sea salt	2–3	1.3 (1–2)	1	~3 (1–4)		3	1 (1–3)

^aWhile source estimates are based on current model knowledge only, the change in transport reflects both model as well as ice core evidence. Deposition changes are based on ice core evidence. Numbers given represent best guesses based on current knowledge, while estimates given in parentheses represent upper and lower limits including all sources of uncertainties.

strong variations in parallel to climate variations with always higher values for cold climate periods. In Table 2 we summarize our best guess estimates on the contribution of individual processes to these overall glacial/interglacial changes. Although local deposition changes on top of the ice sheets due to variations in snow accumulation rates affect the information archived in the ice cores, this effect is rather limited. In case of the low-accumulation areas in East Antarctica the flux is a reliable recorder of atmospheric concentrations overlying the ice sheet, while in Greenland the snow concentration is the better parameter, overestimating the change in atmospheric concentrations only slightly. In any case, local deposition effects cannot explain the order of magnitude changes in sea-salt and mineral dust records in polar ice cores. Thus stronger sources, more efficient transport, and/or less deposition en route must be the main drivers of the observed increases in the sea-salt and mineral dust ice core records during glacial periods.

[56] Provenance and meteorological studies show that the desert regions in China are the main source for dust in Greenland for modern and LGM conditions, while Patagonia is the main source for glacial dust in Antarctica with Australia representing a substantial additional source during the Holocene. A summary of modeling studies supports an increase in global dust emission of a factor of 2–4 in the LGM. However, the different ways different models arrive at that number may allow for a significantly larger glacial increase. The close correspondence of climate and dust records in Greenland with the Chinese loess records (essentially recording local mobilization of dust in the Chinese desert regions) even on millennial timescales [Porter, 2001] shows that such emission changes in the Chinese dust source did occur between the LGM and the Holocene as well as during stadial/interstadial transitions.

[57] For the sea-salt source, significantly less is known. Recent studies on coastal and inland Antarctic aerosol [Hara et al., 2004; Rankin and Wolff, 2003; Wagenbach et al., 1998] show that frost flowers generated during sea ice

formation are an important source for sea salt in addition to the open ocean. We presented a first-order estimate that shows that this source may have been 2–3 times stronger around Antarctica during the glacial; however, at the same time the increased sea ice cover would have reduced the open ocean source. So far, the lack of knowledge on the emission flux from the sea ice source precludes a more quantitative estimate, and systematic studies on sea-salt emission from sea ice are urgently needed to illuminate this problem.

[58] In the case of Greenland sea ice, reconstructions for the North Atlantic do not allow for a quantitative estimate of the sea ice salt source so far. Future refined sea ice modeling efforts for the LGM may identify the locations of sea ice formation, and hence potential sea ice salt production, in the North Atlantic during glacial times. While cyclonic activity over the North Atlantic was generally enhanced during cold periods, the storm tracks were shifted southward. Thus the evidence for an increase in the open ocean sea-salt sources is also not unambiguous. On the basis of modeling results we estimate that the sea ice salt source for Greenland has changed by a factor of 1–3. These estimates do not include a potential underestimation of the gustiness during LGM and stadial climate conditions, which cannot be resolved by circulation models to date. We argue that an additional factor of 2 in the source strength of both sea salt and mineral dust can be explained by the high tail in the wind speed distribution.

[59] Both observational constraints using the size distribution of particulate dust as well as circulation models suggest a possible increase in transport efficiency because of shorter transport times and prolonged atmospheric lifetimes for Greenland. The size of this effect, however, differs, with ice core data indicating a glacial transport-related increase by a factor of 4.5, while models allow for an increase in transport by a factor of 3. For stadial events a transport effect may explain a factor of 3 higher dust concentrations in Greenland compared to interstadials based

on ice core data. For sea salt the transport-induced interglacial/glacial and interstadial/stadial increase may be somewhat smaller in Greenland. In the case of Antarctica neither data nor model evidence indicate a substantial shift in transport intensity during the LGM. In Antarctica, transport time changes are not supported by the available model results, while slightly increased atmospheric lifetimes may have occurred.

[60] A detailed investigation of ion records from Greenland ice cores presented in this study shows that no common linear dependence of logarithmic sea-salt and mineral dust concentrations can be assumed across both warm and cold periods. Instead, the Ca^{2+} record increases more rapidly when temperature conditions fall below a certain threshold. However, separate linear relationships between sea salt and mineral dust are found both for cold and warm periods. An outcome of this analysis is that the regression parameters for the Holocene and the interstadial regimes are very similar. This suggests that the transport regime for the Holocene and the interstadials may not have differed significantly despite the permanent existence of extensive ice sheets during MIS3. Thus we may conclude that the Laurentide and Fennoscandian ice sheets may have had a limited effect on long-range aerosol transport during warm periods; however, the large error in the Holocene regression parameters asks for further studies in this direction. A potential split of the polar jet under conditions of higher baroclinity and higher wind speeds during cold periods is indicated by climate models. This would represent a shortcut for dust transport onto the Greenland ice sheet and may potentially explain the sudden increase in dust relative to sea salt during stadials. Using the latest high-resolution data derived from the NorthGRIP ice core, we were able to show that such a shift from the warm to the cold dust regime occurred in only a few years for the Dansgaard-Oeschger events 3 and 4. The reasons for this rapid switch may be a rapid response in the source strength (e.g., lack of rainfall, higher wind speeds, and increased frequency of dust storm events) or a rapid change in atmospheric transport, as, e.g., a sudden split in the polar jet as described in section 4.2. Because of the potential coupling of transport and source emissions by a sudden shift in location and intensity of the jet stream a separation of the influences of both effects for stadial/interstadial transitions is not straightforward. The aerosol composition in Antarctic ice cores does not reveal a clear linear relationship between logarithmic sea-salt and dust fluxes. We conclude that a common transport effect on sea salt and mineral dust is not the dominating process to explain the glacial/interglacial change in ice core concentrations in Antarctica.

[61] Taking model and data evidence together, we estimate that transport can explain a factor of 3–4.5 change for Greenland dust concentrations during the glacial/interglacial transition and a factor 2–3 change during stadial/interstadial transitions, where the upper limit is based on ice core evidence, while the lower limit summarizes model results. In the case of sea salt the reduced sensitivity of Greenland sea-salt concentrations compared to dust for cold climate periods probably implies a reduced transport effect. We

estimate this effect to explain a factor of 3 change in Greenland sea-salt concentrations for the glacial/interglacial transition and a factor 2 for stadial/interstadial transitions. In Antarctica the model results are limited but may potentially explain a factor of 1–2 change in aerosol fluxes due to changes in transport and atmospheric lifetime. However, complex models suggest only a moderate increase by 20–30%.

[62] Although these estimates of source and transport changes have considerable uncertainties, it shows that both processes are important in Greenland, while source changes clearly dominate in Antarctica. A summary of the increases due to emission changes, transport, and local deposition on the ice sheet is given in Table 2. Although the uncertainties of these best guesses are still large, the observed sea-salt increase may be explained when a significant sea ice salt source is included for Antarctica. Note, however, that knowledge of such a sea ice salt source is still too limited to draw a final conclusion. The LGM dust increase is clearly underestimated by a factor of about 4 in models. Including an increase of dust emissions due to higher gustiness by a moderate factor of 2 and a glacial expansion of the dust source area in southern South America may bring the estimates in line with the ice core observations. For Greenland a similar picture emerges where estimates and observations converge when a sea ice salt source is considered; however, dust is so far strongly underestimated. Because our estimate for the transport effect appears to be on the high side, a significantly stronger change in dust sources is necessary to reconcile model estimates and observations. In the coming years, refined modeling efforts on atmospheric dust and sea-salt formation as well as transport during glacial times will certainly improve our knowledge. A better representation of the wind speed distribution as well as higher-resolution models (increasing local source emissions and decreasing the impact of low-latitude sources to the polar regions because of an improved representation of cyclonic activity) may resolve the discrepancy.

[63] The new NorthGRIP ice core has been analyzed continuously using CFA for the time interval from the latest Eemian to the earliest Holocene. Because of the high snow accumulation and bottom melting at this site this core will allow for seasonal resolution and stratigraphic dating [Rasmussen *et al.*, 2006] for an extended time span. Also, in Antarctica, two new ice cores have been recently drilled within the framework of the European Project for Ice Coring in Antarctica. Results from the Dome C ice core over the last eight glacial cycles [Wolff *et al.*, 2006] have been presented here, and data from the EPICA ice core in Dronning Maud Land are expected soon. The latter represents the first ice core recording changes in environmental conditions (cyclonic activity and sea ice coverage) in the Atlantic sector of the Southern Ocean. Because of its proximity to the Patagonian dust source it will be especially suited to quantify changes in the mineral dust source. In addition, the 2–3 times higher snow accumulation at this site will allow us to resolve seasonal variations in both dust and sea-salt aerosol at least for Holocene conditions [Göktas

et al., 2002; *Sommer et al.*, 2000]. With respect to the recently identified role of sea ice in the sea-salt aerosol budget of Antarctica, current (e.g., Berkner Island or Siple Dome) and future ice cores from coastal regions will strongly enhance our knowledge of regional changes in sea ice coverage. Accordingly, upcoming ice core records from both polar regions will set new standards of aerosol records in both temporal resolution and coverage and are expected to considerably improve our knowledge of aerosol emission and atmospheric transport.

APPENDIX A: ONE-DIMENSIONAL MODEL OF AEROSOL TRANSPORT

[64] In a first-order approximation the change in aerosol concentration $C_{\text{air}}(t)$ of an air parcel along its trajectory is proportional to its concentration itself (assuming no refueling of the air parcel by aerosol formation en route). This assumption also holds for the aerosol concentration of each individual size class of the aerosol $c_{\text{air}}(d, t)$ if we neglect interaction of different size classes in the atmosphere. The latter assumption is sufficiently fulfilled if we only treat aerosol in the accumulation and dispersion mode as is the case for sea salt and mineral dust. The respective partial differential equation can be written as

$$H \frac{dc_{\text{air}}(d, t)}{dt} = -c_{\text{air}} [v_{\text{dry}} + v_{\text{wet}}] = -c_{\text{air}} [kd^2 + \varepsilon A(t)],$$

where the transport time $t = L/u$ is dependent on the intensity of atmospheric circulation (transport velocity u) and its transport patterns (length of the transport path L), H is the typical height of the scavenged air column, v_{dry} and v_{wet} are the dry and wet deposition velocity, respectively. Here v_{dry} is proportional to the square of the particle diameter d for gravitational settling with $k = 8.3 \times 10^7 \text{ m}^{-1} \text{ s}^{-1}$ as used by *Ruth et al.* [2003], while v_{wet} is dependent on the precipitation rate A and the scavenging efficiency ε . We assume that the size fractionating effect of wet deposition is negligible compared to that of dry deposition [*Ruth et al.*, 2003]. Note that all parameters in this equation may, in principle, change along the trajectory; however, it is reasonable to assume that the change in the deposition processes themselves (i.e., k , ε , and H) is small compared to the change in snow precipitation rate $A(t)$. Thus, besides c_{air} , only the precipitation rate is an explicit function of transport time. The equation can be integrated after separation of variables leading to

$$c_{\text{air}}(d, t) = c_{\text{air}}(d, 0) \exp \left[-\frac{kd^2}{H} t - \frac{\varepsilon}{H} \int_0^t A(t) dt \right],$$

where $c_{\text{air}}(d, 0)$ is the air concentration of an individual size class at the source.

[65] Assuming a lognormal distribution of the initial atmospheric size distribution $P_{\text{air}}(\ln d)$ with the maximum of the distribution on a logarithmic scale at diameter μ_{air}

(subsequently referred to as mode) and width σ_{air} , the size distribution is transformed along the transport route according to

$$P_{\text{air}}(\log d, t) = \frac{P_0}{\sqrt{2\pi} \log \sigma_{\text{air},0}} \cdot \exp \left(-\frac{1}{2} \frac{(\log d - \log \mu_{\text{air},0})^2}{\log^2 \sigma_{\text{air},0}} - \frac{t}{H} (kd^2 + \varepsilon A) \right), \quad (\text{A1})$$

where $\mu_{\text{air},0}$ and $\sigma_{\text{air},0}$ are typical parameters of the dust source, which are assumed to be constant and where we replaced the precipitation rate $A(t)$ en route by its average A .

[66] Equation (A1) allows us to estimate the transport time t if changes in the size distribution of particular dust are known from ice core measurements. Analytical determination of the maximum in $P_{\text{air}}(\log d, t)$ leads to

$$\log \frac{\mu_{\text{air}}}{\mu_{\text{air},0}} = -2 \ln 10 \log^2 \sigma_{\text{air},0} \frac{t}{H} k \mu_{\text{air}}^2.$$

If we compare, for example, the mode for cold (LGM or stadials) with the mode for warm (Preboreal or interstadials) conditions, this leads to

$$\log \frac{\mu_{\text{air}}^{\text{cold}}}{\mu_{\text{air}}^{\text{warm}}} = \log \frac{\mu_{\text{air}}^{\text{warm}}}{\mu_{\text{air},0}} \left[\frac{t^{\text{cold}}}{t^{\text{warm}}} \left(\frac{\mu_{\text{air}}^{\text{cold}}}{\mu_{\text{air}}^{\text{warm}}} \right)^2 - 1 \right].$$

Note that this equation is slightly different from the one initially given by *Ruth et al.* [2003]. This results in somewhat smaller values for the ratio $t^{\text{cold}}/t^{\text{warm}}$ in this study. Unfortunately, the atmospheric mode in the past is not known. If we use the measured mode of size distribution in the ice ($\mu^{\text{LGM}} = 1.6 \mu\text{m}$ and $\mu^{\text{PB}} = 1.3 \mu\text{m}$) as a first guess for the atmospheric size distribution and use $\mu_{\text{air},0} = 2.5 \mu\text{m}$, we obtain $t^{\text{LGM}}/t^{\text{PB}} = 0.45$. For stadial/interstadial transitions ($\mu^{\text{S}} = 1.55 \mu\text{m}$ and $\mu^{\text{IS}} = 1.2\text{--}1.4 \mu\text{m}$, where μ^{IS} is not well constrained [*Ruth et al.*, 2003]) this implies $t^{\text{S}}/t^{\text{IS}} = 0.39\text{--}0.69$.

[67] However, the equations given above hold for the size distribution of dust in the atmosphere, while for the measured size distribution in ice the enrichment of large particles due to dry deposition has to be considered

$$P_{\text{ice}}(\log d) \propto P_{\text{air}}(\log d) (kd^2 + \varepsilon A_{\text{ice}}).$$

The same analytical determination of the maximum in the size distribution in the ice leads to

$$\log \frac{\mu_{\text{ice}}^{\text{cold}}}{\mu_{\text{ice}}^{\text{warm}}} = \left(\log \frac{\mu_{\text{ice}}^{\text{warm}}}{\mu_{\text{air},0}} - 2k \ln 10 \log^2 \sigma_{\text{air},0} \frac{\mu_{\text{ice}}^{\text{warm}^2}}{k \mu_{\text{ice}}^{\text{warm}^2} + \varepsilon A_{\text{ice}}^{\text{warm}}} \right) \cdot \left[\frac{t^{\text{cold}}}{t^{\text{warm}}} \left(\frac{\mu_{\text{ice}}^{\text{cold}}}{\mu_{\text{ice}}^{\text{warm}}} \right)^2 - 1 \right] + 2k \ln 10 \log^2 \sigma_{\text{air},0} \cdot \left(\frac{\mu_{\text{ice}}^{\text{cold}^2}}{k \mu_{\text{ice}}^{\text{cold}^2} + \varepsilon A_{\text{ice}}^{\text{cold}}} - \frac{\mu_{\text{ice}}^{\text{warm}^2}}{k \mu_{\text{ice}}^{\text{warm}^2} + \varepsilon A_{\text{ice}}^{\text{warm}}} \right)$$

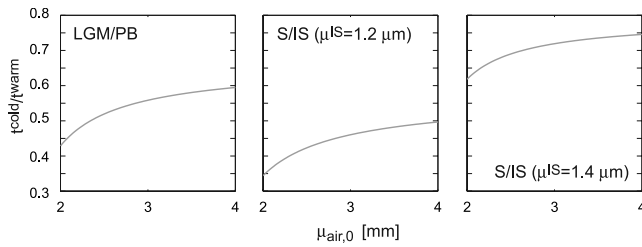


Figure A1. Ratio of transport times for cold versus warm climate conditions as a function of the mode of the initial size distribution. (left) LGM versus Preboreal (PB) ($\mu^{\text{LGM}} = 1.6 \mu\text{m}$, $\sigma^{\text{LGM}} = 1.6 \mu\text{m}$, $\mu^{\text{PB}} = 1.3 \mu\text{m}$, and $\sigma^{\text{PB}} = 2.0 \mu\text{m}$). (middle) Stadial (S) versus interstadial (IS) for the smallest estimate of the mode during IS ($\mu^{\text{S}} = 1.55 \mu\text{m}$, $\sigma^{\text{S}} = 1.6 \mu\text{m}$, $\mu^{\text{IS}} = 1.2 \mu\text{m}$, and $\sigma^{\text{IS}} = 2.0 \mu\text{m}$). (right) S versus IS for largest estimate of the mode during IS ($\mu^{\text{S}} = 1.55 \mu\text{m}$, $\sigma^{\text{S}} = 1.6 \mu\text{m}$, $\mu^{\text{IS}} = 1.4 \mu\text{m}$, and $\sigma^{\text{IS}} = 2.0 \mu\text{m}$).

While this determines $t^{\text{cold}}/t^{\text{warm}}$ analytically, it is dependent on $\sigma_{\text{air},0}$, which again is a priori not known. For example, calculating the change in transport times in the LGM compared to the PB time period ($A_{\text{ice}}^{\text{LGM}} = 0.05$ meters water equivalent (mwe)/yr and $A_{\text{ice}}^{\text{PB}} = 0.2$ mwe/yr [Cuffey and Clow, 1997]), this equation leads to $t^{\text{LGM}}/t^{\text{PB}} = 0.81$ for $\sigma_{\text{air},0} = 4 \mu\text{m}$ but $t^{\text{LGM}}/t^{\text{PB}} = 0.51$ for $\sigma_{\text{air},0} = 1.7 \mu\text{m}$ ($k = 83 \mu\text{m}^{-1} \text{s}^{-1}$ and $\varepsilon = 1 \times 10^6$ as used by Ruth et al. [2003]). For stadial/interstadial transitions, where we estimated $A_{\text{ice}}^{\text{IS}} = 0.1$ mwe/yr [Cuffey and Clow, 1997] and using $\sigma_{\text{air},0} = 1.7 \mu\text{m}$, we obtain $t^{\text{S}}/t^{\text{IS}} = 0.43\text{--}0.73$ dependent on the choice of μ^{IS} between 1.2 and 1.4 μm .

[68] If we assume that the size distribution at the time of deposition is also approximately lognormal, we can also express μ_{air} in terms of μ_{ice} with

$$\log \frac{\mu_{\text{ice}}}{\mu_{\text{air}}} = 2k \ln 10 \log^2 \sigma_{\text{air}} \frac{\mu_{\text{ice}}^2}{k\mu_{\text{ice}}^2 + \varepsilon A_{\text{ice}}}$$

Again, we need the width of the size distribution in the air, which is not known a priori; however, the change in the width between ice and air over the ice sheet is small and does not have a strong effect on the result. So in the following, we assume that $\sigma_{\text{air}} \approx \sigma_{\text{ice}}$. Then we can estimate μ_{air} from μ_{ice} and use the width-independent formula for $\log(\mu_{\text{air}}^{\text{cold}}/\mu_{\text{air}}^{\text{warm}})$ given above to calculate $t^{\text{cold}}/t^{\text{warm}}$. In this case we obtain the values summarized in Figure A1 as a function of the mode of the initial size distribution, which is also not exactly known a priori. Here we will use $\mu_{\text{air},0} = 2.5 \mu\text{m}$. Note, however, that $t^{\text{cold}}/t^{\text{warm}}$ will vary only by ± 0.05 within reasonable bounds for the mode of the initial size distribution. Using these values, we arrive at $t^{\text{LGM}}/t^{\text{PB}} = 0.52$ and $t^{\text{S}}/t^{\text{IS}} = 0.43\text{--}0.69$, dependent on the value taken to be representative for the mode during interstadials. As a best guess we use $t^{\text{S}}/t^{\text{IS}} = 0.65$ at the upper end of the interstadial mode.

[69] **ACKNOWLEDGMENTS.** We thank all participants in the field and laboratory for their commitment in collecting high-accuracy data under adverse conditions. We thank M. Bigler and S. Johnsen for providing unpublished high-resolution ion and

isotope data from the NorthGRIP ice core. The NorthGRIP project is directed and organized by the Department of Geophysics at the Niels Bohr Institute for Astronomy, Physics and Geophysics, University of Copenhagen. It is supported by funding agencies in Denmark, Belgium, France, Germany, Iceland, Japan, Sweden, Switzerland, and the United States of America. The European Project for Ice Coring in Antarctica (EPICA), a joint ESF (European Science Foundation)/EU scientific program, is funded by the European Commission (EPICA-MIS) and by national contributions from Belgium, Denmark, France, Germany, Italy, Netherlands, Norway, Sweden, Switzerland, and the United Kingdom. H.F. has been funded by the junior research group grant RESPIC by the German Secretary for Education and Research (BMBF) within the German climate research program DEKLIM.

[70] The Editor responsible for this paper was Ian Fairchild. He thanks Martin Sharp and an anonymous technical reviewer.

REFERENCES

- Alley, R. B., et al. (1993), Abrupt increase in Greenland snow accumulation at the end of the Younger Dryas event, *Nature*, 362, 527–529.
- Alley, R. B., R. C. Finkel, K. Nishiizumi, S. Anandkrishnan, C. A. Shuman, G. Mershon, G. A. Zielinski, and P. A. Mayewski (1995), Changes in continental and sea-salt atmospheric loadings in central Greenland during the most recent deglaciation: Model-based estimates, *J. Glaciol.*, 41, 503–514.
- Andersen, K. K., and P. D. Ditlevsen (1998), Glacial/interglacial variations of meridional transport and washout of dust: A one-dimensional model, *J. Geophys. Res.*, 103, 8955–8962.
- Andersen, K. K., A. Armengaud, and C. Genthon (1998), Atmospheric dust under glacial and interglacial conditions, *Geophys. Res. Lett.*, 25, 2281–2284.
- Basile, I., F. E. Grousset, M. Revel, J. R. Petit, P. E. Biscaye, and N. I. Barkov (1997), Patagonian origin of glacial dust deposited in East Antarctica (Vostok and Dome C) during glacial stages 2, 4 and 6, *Earth Planet. Sci. Lett.*, 146, 573–589.
- Bigler, M., R. Röthlisberger, F. Lambert, T. F. Stocker, and D. Wagenbach (2006), Aerosol deposited in East Antarctica over the last glacial cycle: Detailed apportionment of continental and sea-salt contributions, *J. Geophys. Res.*, 111, D08205, doi:10.1029/2005JD006469.
- Biscaye, P. E., F. E. Grousset, M. Revel, S. V. D. Gaast, G. A. Zielinski, A. Vaars, and G. Kukla (1997), Asian provenance of glacial dust (Stage 2) in the GISP2 ice core, Summit, Greenland, *J. Geophys. Res.*, 102, 26,765–26,781.
- Blunier, T., and E. J. Brook (2001), Timing of millennial-scale climate change in Antarctica and Greenland during the last glacial period, *Science*, 291, 109–112.
- Blunier, T., J. Schwander, B. Stauffer, T. Stocker, A. Dällenbach, A. Indermühle, J. Tschumi, J. Chappellaz, D. Raynaud, and J.-M. Barnola (1997), Timing of the Antarctic Cold Reversal and the atmospheric CO₂ increase with respect to the Younger Dryas event, *Geophys. Res. Lett.*, 24, 2683–2686.
- Blunier, T., et al. (1998), Asynchrony of Antarctic and Greenland climate change during the last glacial period, *Nature*, 394, 739–743.
- Bond, G., W. Broecker, S. Johnsen, J. McManus, L. Labeyrie, J. Jouzel, and G. Bonani (1993), Correlations between records from North Atlantic sediments and Greenland ice, *Nature*, 365, 143–147.
- Bory, A. J.-M., P. E. Biscaye, A. M. Piotrowski, and J. P. Steffensen (2003), Regional variability of ice core dust composition and provenance in Greenland, *Geochem. Geophys. Geosyst.*, 4(12), 1107, doi:10.1029/2003GC000627.
- Boutroun, C. (1979), Trace element content of Greenland snows along an east-west transect, *Geochim. Cosmochim. Acta*, 43, 1253–1258.

- Bowen, H. J. M. (1979), *Environmental Chemistry of the Elements*, Elsevier, New York.
- Boyd, P. W., et al. (2000), A mesoscale phytoplankton bloom in the polar Southern Ocean stimulated by iron fertilization, *Nature*, *407*, 695–702.
- Broecker, W. S. (1998), Paleocirculation during the last deglaciation: A bipolar seesaw, *Paleoceanography*, *13*, 119–121.
- Bromwich, D. H., E. R. Toracinta, H. Wei, R. J. Oglesby, J. L. Fastook, and T. J. Hughes (2004), Polar MM5 simulations of the winter climate of the Laurentide Ice Sheet at the LGM, *J. Clim.*, *17*, 3415–3433.
- Bush, A. B. G., and S. G. H. Philander (1999), The climate of the Last Glacial Maximum: Results from a coupled atmosphere-ocean general circulation model, *J. Geophys. Res.*, *104*, 24,509–24,525.
- Chen, Q.-S., D. A. Bromwich, and L. Bai (1997), Precipitation over Greenland retrieved by a dynamic method and its relation to cyclonic activity, *J. Clim.*, *10*, 539–570.
- Chylek, P., G. Lesins, and U. Lohmann (2001), Enhancement of dust source area during past glacial periods due to changes of the Hadley circulation, *J. Geophys. Res.*, *106*, 18,477–18,485.
- CLIMAP Project Members (1976), The surface of the ice-age earth, *Science*, *191*, 1131–1144.
- CLIMAP Project Members (Ed.) (1981), Seasonal reconstructions of the Earth's surface at the last glacial maximum, *Geol. Soc. Am. Map Chart Ser.*, MC-3, 1–18.
- Cooke, D. W., and J. D. Hays (1982), Estimates of Antarctic Ocean seasonal sea-ice cover during glacial intervals, in *Antarctic Geosciences*, edited by C. Craddock, pp. 1017–1025, Univ. of Wis. Press, Madison.
- Crosta, X., J. J. Pichon, and L. H. Burckle (1998), Application of modern analog technique to marine Antarctic diatoms: Reconstruction of maximum sea-ice extent at the last glacial maximum, *Paleoceanography*, *13*, 284–297.
- Cuffey, C. M., and G. D. Clow (1997), Temperature, accumulation, and ice sheet elevation in central Greenland through the last deglacial transition, *J. Geophys. Res.*, *102*, 26,383–26,396.
- Dansgaard, W., J. W. C. White, and S. J. Johnsen (1989), The abrupt termination of the Younger Dryas climate event, *Nature*, *339*, 532–534.
- de Angelis, M., N. I. Barkov, and V. N. Petrov (1992), Sources of continental dust over Antarctica during the last glacial cycle, *J. Atmos. Chem.*, *14*, 233–244.
- de Angelis, M., J. P. Steffensen, M. Legrand, H. Clausen, and C. Hammer (1997), Primary aerosol (sea salt and soil dust) deposited in Greenland ice during the last climatic cycle: Comparison with east Antarctic records, *J. Geophys. Res.*, *102*, 26,681–26,698.
- Delmonte, B., J. R. Petit, and V. Maggi (2002), Glacial to Holocene implications of the new 27,000-year dust record from the EPICA Dome C (East Antarctica) ice core, *Clim. Dyn.*, *18*, 647–660.
- Delmonte, B., I. Basile-Doelsch, J. R. Petit, V. Maggi, M. Revel-Rolland, A. Michard, and F. Grousset (2004a), Comparing the EPICA and Vostok dust records during the last 220,000 years: Stratigraphical correlation and provenance in glacial periods, *Earth Sci. Rev.*, *66*, 63–87.
- Delmonte, B., J. R. Petit, K. K. Andersen, I. Basile-Doelsch, V. Maggi, and V. Lipenkov (2004b), Dust size evidence for opposite regional atmospheric circulation changes over East Antarctica during the last climatic transition, *Clim. Dyn.*, *23*, 427–438.
- Delmonte, B., J. R. Petit, I. Basile-Doelsch, E. Jagoutz, and V. Maggi (2007), Late Quaternary interglacials in East Antarctica from ice core dust records, in *The Climate of the Past Interglacials*, edited by F. Sirocko et al., pp. 53–73, Elsevier, New York.
- Dentener, F. J., G. R. Carmichael, Y. Zhang, J. Lelieveld, and P. J. Crutzen (1996), Role of mineral aerosol as a reactive surface in the global troposphere, *J. Geophys. Res.*, *101*, 22,869–22,889.
- EPICA Community Members (2004), Eight glacial cycles from an Antarctic ice core, *Nature*, *429*, 623–628.
- EPICA Community Members (2006), One-to-one coupling of glacial climate variability in Greenland and Antarctica, *Nature*, *444*, 195–198.
- Falkowski, P., et al. (2000), The global carbon cycle: A test of our knowledge of Earth as a system, *Science*, *290*, 291–296.
- Fischer, H., and B. Mieding (2005), A 1000-year ice core record of annual to multidecadal variations in atmospheric circulation over the North Atlantic, *Clim. Dyn.*, *25*, 65–74, doi:10.1007/s00382_00005_00011_x.
- Fischer, H., and D. Wagenbach (1996), Large-scale spatial trends in recent firn chemistry along an east-west transect through central Greenland, *Atmos. Environ.*, *30*, 3227–3238.
- Fischer, H., D. Wagenbach, and J. Kipfstuhl (1998a), Sulfate and nitrate firn concentrations on the Greenland ice sheet: 1. Large-scale geographical deposition changes, *J. Geophys. Res.*, *103*, 21,927–21,934.
- Fischer, H., D. Wagenbach, and J. Kipfstuhl (1998b), Sulfate and nitrate firn concentrations on the Greenland ice sheet: 2. Temporal anthropogenic deposition changes, *J. Geophys. Res.*, *103*, 21,935–21,942.
- Fischer, H., F. Traufetter, H. Oerter, R. Weller, and H. Miller (2004), Prevalence of the Antarctic Circumpolar Wave over the last two millennia recorded in Dronning Maud Land ice, *Geophys. Res. Lett.*, *31*, L08202, doi:10.1029/2003GL019186.
- Fuhrer, K., A. Neftel, M. Ankin, and V. Maggi (1993), Continuous measurements of hydrogen peroxide, formaldehyde, calcium and ammonium concentrations along the new GRIP ice core from Summit, central Greenland, *Atmos. Environ.*, *27*, 1873–1880.
- Fuhrer, K., E. W. Wolff, and S. J. Johnsen (1999), Timescales for dust variability in the Greenland Ice Core Project (GRIP) ice core in the last 100,000 years, *J. Geophys. Res.*, *104*, 31,043–31,052.
- Gabrielli, P., et al. (2005), Meteoric smoke fallout over the Holocene epoch revealed by iridium and platinum in Greenland ice, *Nature*, *432*, 1011–1014.
- Ganopolski, A., S. Rahmstorf, V. Petoukhov, and M. Claussen (1998), Simulation of modern and glacial climates with a coupled global model of intermediate complexity, *Nature*, *391*, 351–356.
- Genthon, C. (1992), Simulations of desert dust and sea-salt aerosols in Antarctica with a general circulation model of the atmosphere, *Tellus, Ser. B*, *44*, 371–389.
- Gersonde, R., et al. (2003), Last glacial sea surface temperatures and sea-ice extent in the Southern Ocean (Atlantic-Indian sector): A multiproxy approach, *Paleoceanography*, *18*(3), 1061, doi:10.1029/2002PA000809.
- Gersonde, R., X. Crosta, A. Abelmann, and L. Armand (2005), Sea-surface temperature and sea ice distribution of the Southern Ocean at the EPILOG Last Glacial Maximum—A circum-Antarctic view based on siliceous microfossil records, *Quat. Sci. Rev.*, *24*, 869–896.
- Gillette, D. A., and R. Passi (1988), Modeling dust emission caused by wind erosion, *J. Geophys. Res.*, *93*, 14,233–14,242.
- Gillette, D. A., J. Adams, A. Endo, and D. Smith (1980), Threshold velocities for input of soil particles into the air by desert soil, *J. Geophys. Res.*, *85*, 5621–5630.
- Göktas, F., H. Fischer, H. Oerter, R. Weller, S. Sommer, and H. Miller (2002), A glacio-chemical characterisation of the new EPICA deep drilling site on Amundsenisen, Dronning Maud Land, Antarctica, *Ann. Glaciol.*, *35*, 347–354.
- Gong, S. L., X. Y. Zhang, T. L. Zhao, I. G. McKendry, D. A. Jaffe, and N. M. Lu (2003), Characterization of soil dust aerosol in China and its transport and distribution during 2001 ACE-Asia: 2. Model simulation and validation, *J. Geophys. Res.*, *108*(D9), 4262, doi:10.1029/2002JD002633.
- Groote, P. M., M. Stuiver, J. W. C. White, S. Johnsen, and J. Jouzel (1993), Comparison of oxygen isotope records from the GISP2 and GRIP Greenland ice cores, *Nature*, *366*, 552–554.
- Grousset, F. E., P. E. Biscaye, M. Revel, J.-R. Petit, K. Pye, S. Joussaume, and J. Jouzel (1992), Antarctic (Dome C) ice core dust at 18 k.y. B.P.: Isotopic constraints on origins, *Earth Planet. Sci. Lett.*, *111*, 175–182.

- Guelle, W., M. Schulz, and Y. Balkanski (2001), Influence of the source formulation on modeling the atmospheric distribution of sea salt aerosol, *J. Geophys. Res.*, *106*, 27,509–27,524.
- Guilderson, T. P., L. H. Burckle, S. Hemming, and W. R. Peltier (2000), Late Pleistocene sea level variations derived from the Argentine Shelf, *Geochem. Geophys. Geosyst.*, *1*(12), doi:10.1029/2000GC000098.
- Hammer, C. U., H. Clausen, and W. Dansgaard (1985), Continuous impurity analysis along the Dye 3 deep ice core, in *Greenland Ice Core: Geophysics, Geochemistry and the Environment*, *Geophys. Monogr. Ser.*, vol. 33, edited by C. C. Langway et al., pp. 90–94, AGU, Washington, D. C.
- Hammer, C. U., H. B. Clausen, and C. C. Langway Jr. (1997), 50,000 years of recorded global volcanism, *Clim. Change*, *35*, 1–15.
- Hansson, M. E. (1994), The Renland ice core: A Northern Hemisphere record of aerosol composition over 120,000 years, *Tellus, Ser. B*, *46*, 390–418.
- Hara, K., K. Osada, M. Kido, M. Hayashi, K. Matsunaga, Y. Iwasaka, T. Yamanouchi, G. Hashida, and T. Fukatsu (2004), Chemistry of sea-salt particles and inorganic halogen species in Antarctic regions: Compositional differences between coastal and inland stations, *J. Geophys. Res.*, *109*, D20208, doi:10.1029/2004JD004713.
- Intergovernmental Panel on Climate Change (2001), *Climate Change 2001: The Scientific Basis: Contribution of Working Group I to the Third Assessment Report of the Intergovernmental Panel on Climate Change*, edited by J. T. Houghton et al., 881 pp., Cambridge Univ. Press, New York.
- Johnsen, S. J., H. B. Clausen, W. Dansgaard, K. Fuhrer, N. Gundestrup, C. U. Hammer, P. Iversen, J. Jouzel, B. Stauffer, and J. P. Steffensen (1992), Irregular glacial interstadials recorded in a new Greenland ice core, *Nature*, *359*, 311–313.
- Joussaume, S. (1990), Three-dimensional simulation of the atmospheric cycle of desert dust particles using a general circulation model, *J. Geophys. Res.*, *95*, 1909–1941.
- Joussaume, S. (1993), Paleoclimatic tracers: An investigation using an atmospheric general circulation model under ice age conditions: 1. Desert dust, *J. Geophys. Res.*, *98*, 2767–2805.
- Kahl, J. D. W., D. A. Martinez, H. Kuhns, C. Davidson, J.-L. Jaffrezo, and J. M. Harris (1997), Air mass trajectories to Summit, Greenland: A 44-year climatology and some episodic events, *J. Geophys. Res.*, *102*, 26,861–26,876.
- Knutti, R., J. Flückiger, T. F. Stocker, and A. Timmermann (2004), Strong hemispheric coupling of glacial climate through freshwater discharge and ocean circulation, *Nature*, *430*, 851–856.
- Kohfeld, K., and S. P. Harrison (2001), DIRTMAP: The geological record of dust, *Earth Sci. Rev.*, *54*, 81–114.
- Kreutz, K., P. A. Mayewski, L. D. Pittalwala, L. D. Meeker, M. S. Twickler, and S. I. Whitlow (2000), Sea level pressure variability in the Amundsen Sea region inferred from a West Antarctic glaciochemical record, *J. Geophys. Res.*, *105*, 4047–4059.
- Krinner, G., and C. Genthon (1998), GCM simulation of the Last Glacial Maximum surface climate of Greenland and Antarctica, *Clim. Dyn.*, *14*, 741–758.
- Legrand, M. (1987), Chemistry of Antarctic snow and ice, *J. Phys., CI*, 77–86.
- Legrand, M. (1995), Sulphur-derived species in polar ice: A review, in *Ice Core Studies of Global Biogeochemical Cycles*, edited by R. J. Delmas, pp. 91–119, Springer, New York.
- Legrand, M. R., and R. J. Delmas (1988), Formation of HCl in the Antarctic atmosphere, *J. Geophys. Res.*, *93*, 7153–7168.
- Legrand, M., S. Preunkert, D. Wagenbach, and H. Fischer (2002), Seasonally resolved Alpine and Greenland ice core records of anthropogenic HCl emissions over the 20th century, *J. Geophys. Res.*, *107*(D12), 4139, doi:10.1029/2001JD001165.
- Lunt, D. J., and P. J. Valdes (2001), Dust transport to Dome C, Antarctica, at the Last Glacial Maximum and present day, *Geophys. Res. Lett.*, *28*, 295–298.
- Maggi, V. (1997), Mineralogy of atmospheric microparticles deposited along the Greenland Ice Core Project ice core, *J. Geophys. Res.*, *102*, 26,725–26,734.
- Mahowald, N., K. Kohfeld, M. Hansson, Y. Balkanski, S. P. Harrison, I. C. Prentice, M. Schulz, and H. Rodhe (1999), Dust sources and deposition during the last glacial maximum and current climate: A comparison of model results with paleodata from ice cores and marine sediments, *J. Geophys. Res.*, *104*, 18,895–18,916.
- Marticorena, B., and G. Bergametti (1995), Modeling the atmospheric dust cycle: 1. Design of a soil-derived dust emission scheme, *J. Geophys. Res.*, *100*, 16,415–16,430.
- Martin, J. (1990), Glacial-interglacial CO₂ change: The iron hypothesis, *Paleoceanography*, *5*, 1–13.
- Mayewski, P. A., M. J. Spencer, W. B. Lyons, and M. S. Twickler (1987), Seasonal and spatial trends in south Greenland snow chemistry, *Atmos. Environ.*, *21*, 863–869.
- Mayewski, P. A., et al. (1994), Changes in atmospheric circulation and ocean ice cover over the North Atlantic during the last 41,000 years, *Science*, *263*, 1747–1751.
- Mayewski, P. A., et al. (1996), Climate change during the last deglaciation in Antarctica, *Science*, *272*, 1636–1638.
- Mayewski, P. A., L. D. Meeker, M. Twickler, S. Whitlow, Q. Yang, W. B. Lyons, and M. Prentice (1997), Major features and forcing of high-latitude Northern Hemisphere atmospheric circulation using a 110,000-year-long glaciochemical series, *J. Geophys. Res.*, *102*, 26,345–26,366.
- McManus, J. F., D. W. Oppo, and J. L. Cullen (1999), A 0.5-million-year record of millennial climate variability in the North Atlantic, *Science*, *283*, 971–975.
- Meese, D. A., A. J. Gow, P. M. Grootes, P. A. Mayewski, M. Ram, M. Stuiver, K. C. Taylor, E. D. Waddington, and G. A. Zielinski (1994), The accumulation record from the GISP2 core as an indicator of climate change throughout the Holocene, *Science*, *266*, 1680–1682.
- Monahan, E. C., D. E. Spiel, and K. L. Davidson (1986), A model of marine aerosol generation via whitecaps and wave disruption, in *Oceanic Whitecaps and Their Role in Air-Sea Exchange Processes*, edited by E. C. Monahan and G. Niocaill, pp. 167–174, Springer, New York.
- Noone, D., J. Turner, and R. Mulvaney (1999), Atmospheric signals and characteristics of accumulation in Dronning Maud Land, Antarctica, *J. Geophys. Res.*, *104*, 19,191–19,211.
- North Greenland Ice Core Project Members (2004), High resolution climate record of the Northern Hemisphere reaching into the last interglacial period, *Nature*, *431*, 147–151.
- Peltier, W. R. (1994), Ice age paleotopography, *Science*, *265*, 195–201.
- Petit, J. R., L. Mounier, J. Jouzel, Y. S. Korotkevich, V. Kotlyakov, and C. Lorius (1990), Paleoclimatological and chronological implications of the Vostok core dust record, *Nature*, *343*, 429–436.
- Petit, J. R., et al. (1999), Climate and atmospheric history of the past 420,000 years from the Vostok ice core, Antarctica, *Nature*, *399*, 429–436.
- Pflaumann, U., et al. (2003), Glacial North Atlantic: Sea-surface conditions reconstructed by GLAMAP 2000, *Paleoceanography*, *18*(3), 1065, doi:10.1029/2002PA000774.
- Porter, S. C. (2001), Chinese loess record of monsoon climate during the last glacial-interglacial cycle, *Earth Sci. Rev.*, *54*, 115–128.
- Porter, S. C., and Z. An (1995), Correlation between climate events in the North Atlantic and China during the last glaciation, *Nature*, *375*, 305–308.
- Prospero, J. M., P. Ginoux, O. Torres, S. E. Nicholson, and T. E. Gill (2002), Environmental characterization of global sources of atmospheric soil dust identified with the Nimbus 7 total ozone mapping spectrometer (TOMS) absorbing aerosol product, *Rev. Geophys.*, *40*(1), 1002, doi:10.1029/2000RG000095.

- Ram, M., and G. Koenig (1997), Continuous dust concentration profile of pre-Holocene ice from the Greenland Ice Sheet Project 2 ice core: Dust stadials, interstadials, and the Eemian, *J. Geophys. Res.*, *102*, 26,641–26,648.
- Rankin, A. M., and E. W. Wolff (2003), A year-long record of size-segregated aerosol composition at Halley, Antarctica, *J. Geophys. Res.*, *108*(D24), 4775, doi:10.1029/2003JD003993.
- Rankin, A. M., V. Auld, and E. W. Wolff (2000), Frost flowers as a source of fractionated sea salt aerosol in the polar regions, *Geophys. Res. Lett.*, *27*, 3469–3472.
- Rasmussen, S. O., et al. (2006), A new Greenland ice core chronology for the last glacial termination, *J. Geophys. Res.*, *111*, D06102, doi:10.1029/2005JD006079.
- Raynaud, D., J. Chappellaz, C. Ritz, and P. Martinerie (1997), Air content along the Greenland Ice Core Project core: A record of surface climatic parameters and elevation in central Greenland, *J. Geophys. Res.*, *102*, 26,607–26,613.
- Rea, D. K. (1994), The paleoclimatic record provided by eolian deposition in the deep sea: The geological history of wind, *Rev. Geophys.*, *32*, 159–195.
- Reader, M. C., and N. McFarlane (2003), Sea-salt aerosol distribution during the Last Glacial Maximum and its implications for mineral dust, *J. Geophys. Res.*, *108*(D8), 4253, doi:10.1029/2002JD002063.
- Reader, M. C., I. Fung, and N. McFarlane (1999), The mineral dust aerosol cycle during the Last Glacial Maximum, *J. Geophys. Res.*, *104*, 9381–9398.
- Reijmer, C. H., and M. R. van den Broeke (2000), Moisture sources of precipitation in western Dronning Maud Land, Antarctica, *Antarct. Sci.*, *13*, 210–220.
- Reijmer, C. H., M. R. van den Broeke, and M. P. Scheele (2002), Air parcel trajectories to five deep drilling locations on Antarctica, based on the ERA-15 data set, *J. Clim.*, *15*, 1957–1968.
- Revel-Rolland, M., P. De Dekker, B. Delmonte, P. P. Hesse, J. W. Magee, I. Basile-Doelsch, F. Grousset, and D. Bosch (2006), Eastern Australia: A possible source of dust in East Antarctica interglacial ice, *Earth Planet. Sci. Lett.*, *249*, 1–13.
- Röthlisberger, R., M. Bigler, M. Hutterli, S. Sommer, B. Stauffer, H. G. Junghans, and D. Wagenbach (2000), Technique for continuous high-resolution analysis of trace substances in firn and ice cores, *Environ. Sci. Technol.*, *34*, 338–342.
- Röthlisberger, R., R. Mulvaney, E. W. Wolff, M. Hutterli, M. Bigler, S. Sommer, and J. Jouzel (2002), Dust and sea-salt variability in central East Antarctica (Dome C) over the last 45 kyr and its implications for southern high-latitude climate, *Geophys. Res. Lett.*, *29*(20), 1963, doi:10.1029/2002GL015186.
- Röthlisberger, R., R. Mulvaney, E. W. Wolff, M. A. Hutterli, M. Bigler, M. de Angelis, M. E. Hansson, J. P. Steffensen, and R. Udisti (2003), Limited dechlorination of sea-salt aerosols during the last glacial period: Evidence from the European Project for Ice Coring in Antarctica (EPICA) Dome C ice core, *J. Geophys. Res.*, *108*(D16), 4526, doi:10.1029/2003JD003604.
- Ruth, U., D. Wagenbach, J. P. Steffensen, and M. Bigler (2003), Continuous record of microparticle concentration and size distribution in the central Greenland NGRIP ice core during the last glacial period, *J. Geophys. Res.*, *108*(D3), 4098, doi:10.1029/2002JD002376.
- Sarnthein, M., U. Pflaumann, and M. Weinelt (2003), Past extent of sea ice in the northern North Atlantic inferred from foraminiferal paleotemperature estimates, *Paleoceanography*, *18*(2), 1047, doi:10.1029/2002PA000771.
- Schulz, H., U. von Rad, and H. Erlenkeuser (1998), Correlation between Arabian Sea and Greenland climate oscillations of the past 110,000 years, *Nature*, *393*, 54–57.
- Schwander, J., J. Jouzel, C. U. Hammer, J. R. Petit, R. Udisti, and E. Wolff (2001), A tentative chronology for the EPICA Dome Concordia ice core, *Geophys. Res. Lett.*, *28*, 4243–4246.
- Shin, S.-I., Z. Liu, B. Otto-Bliesner, E. C. Brady, J. E. Kutzbach, and S. P. Harrison (2003), A simulation of the Last Glacial Maximum climate using the NCAR-CCSM, *Clim. Dyn.*, *20*, 127–151.
- Siggaard-Andersen, M.-L. (2004), Analysis of soluble ions from dust and sea salt over the last glacial cycle in polar deep ice cores, Ph.D. thesis, Univ. of Bremen, Bremen, Germany.
- Simmonds, I., and K. Keay (2000), Mean Southern Hemisphere extratropical cyclone behavior in the 40-year NCEP-NCAR re-analysis, *J. Clim.*, *13*, 873–885.
- Sommer, S., D. Wagenbach, R. Mulvaney, and H. Fischer (2000), Glacio-chemical study covering the past 2 kyr on three ice cores from Dronning Maud Land, Antarctica 2. Seasonally resolved chemical records, *J. Geophys. Res.*, *105*, 29,423–29,433.
- Steffensen, J. P. (1985), Microparticles in snow from the south Greenland Ice Sheet, *Tellus, Ser. B*, *37*, 286–295.
- Steffensen, J. P. (1988), Analysis of the seasonal variation in dust, Cl^- , NO_3^- , and SO_4^{2-} in two central Greenland firn cores, *Ann. Glaciol.*, *10*, 171–177.
- Steffensen, J. P. (1997), The size distribution of microparticles from selected segments of the Greenland Ice Core Project ice core representing different climatic periods, *J. Geophys. Res.*, *102*, 26,755–26,763.
- Stenni, B., V. Masson-Delmotte, S. Johnsen, J. Jouzel, A. Longinelli, E. Monnin, R. Röthlisberger, and E. Selmo (2001), An oceanic cold reversal during the last deglaciation, *Science*, *293*, 2074–2077.
- Stocker, T., and S. Johnsen (2003), A minimum thermodynamic model of the bipolar seesaw, *Paleoceanography*, *18*(4), 1087, doi:10.1029/2003PA000920.
- Sugden, D. E., M. J. Bentley, C. J. Fogwill, N. R. J. Hulton, R. D. McCulloch, and R. S. Purves (2005), Late-glacial glacier events in southernmost South America, *Geogr. Ann., Ser. A*, *87*, 273–288.
- Sun, J. (2002), Provenance of loess material and formation of loess deposits on the Chinese Loess Plateau, *Earth Planet. Sci. Lett.*, *203*, 845–859.
- Svensson, A., P. E. Biscaye, and F. E. Grousset (2000), Characterization of late glacial continental dust in the Greenland Ice Core Project ice core, *J. Geophys. Res.*, *105*, 4637–4656.
- Swap, R., M. Garstang, S. Greco, R. W. Talbot, and P. Kallberg (1992), Saharan dust in the Amazon Basin, *Tellus, Ser. B*, *144*, 133–149.
- Taylor, K. C., et al. (1997), The Holocene–Younger Dryas transition recorded at Summit, Greenland, *Science*, *278*, 825–827.
- Tegen, I. (2003), Modeling the mineral dust aerosol cycle in the climate system, *Quat. Sci. Rev.*, *22*, 1821–1834.
- Tegen, I., and I. Fung (1994), Modeling of mineral dust in the atmosphere: Sources, transport, and optical thickness, *J. Geophys. Res.*, *99*, 22,897–22,914.
- Tegen, I., and D. Rind (2000), Influence of the latitudinal temperature gradient on soil dust composition and deposition in Greenland, *J. Geophys. Res.*, *105*, 7199–7212.
- Tegen, I., A. Lacis, and I. Fung (1996), The influence on climate forcing of mineral aerosols from disturbed soils, *Nature*, *380*, 419–422.
- Thompson, L. G., E. Mosley-Thompson, M. E. Davis, P.-N. Lin, K. A. Henderson, J. Cole-Dai, J. F. Bolzan, and K.-B. Liu (1995), Late glacial stage and Holocene tropical ice core records from Huascarán, Peru, *Science*, *269*, 46–50.
- Thompson, L. G., T. Yao, M. E. Davis, K. A. Henderson, E. Mosley-Thompson, P.-N. Lin, J. Beer, H.-A. Synal, J. Cole-Dai, and J. F. Bolzan (1997), Tropical climate instability: The last glacial cycle from a Qinghai-Tibetan ice core, *Science*, *276*, 1821–1825.
- Thompson, L. G., et al. (1998), A 25,000-year tropical climate history from Bolivian ice cores, *Science*, *282*, 1858–1864.
- Timmreck, C., and M. Schulz (2004), Significant dust simulation differences in nudged and climatological operation mode of the AGCM ECHAM, *J. Geophys. Res.*, *109*, D13202, doi:10.1029/2003JD004381.

- Wagenbach, D., F. Ducroz, R. Mulvaney, L. Keck, A. Minikin, M. Legrand, J. S. Hall, and E. W. Wolff (1998), Sea-salt aerosol in coastal Antarctic regions, *J. Geophys. Res.*, *103*, 10,961–10,974.
- Watson, A. J., D. C. E. Bakker, A. J. Ridgwell, P. W. Boyd, and C. S. Law (2000), Effect of iron supply on Southern Ocean CO₂ uptake and implications for glacial atmospheric CO₂, *Nature*, *407*, 730–733.
- Werner, M., I. Tegen, S. P. Harrison, K. Kohfeld, I. C. Prentice, Y. Balkanski, H. Rodhe, and C. Roelandt (2002), Seasonal and interannual variability of the mineral dust cycle under present and glacial conditions, *J. Geophys. Res.*, *107*(D24), 4744, doi:10.1029/2002JD002365.
- Winckler, G., and H. Fischer (2006), 30,000 years of cosmic dust in Antarctic ice, *Science*, *313*, 491.
- Wolff, E. W., A. M. Rankin, and R. Röthlisberger (2003), An ice core indicator of Antarctic sea ice production?, *Geophys. Res. Lett.*, *30*(22), 2158, doi:10.1029/2003GL018454.
- Wolff, E. W., et al. (2006), Southern Ocean sea ice, DMS production and iron flux over the last eight glacial cycles, *Nature*, *440*, 491–496.
- Xiao, J., and Z. An (1999), Three large shifts in East Asian Monsoon circulation indicated by loess-paleosol sequences in China and late Cenozoic deposits in Japan, *Palaogeogr. Palaeoclimatol. Palaeoecol.*, *154*, 179–189.
- Yung, Y., T. Lee, C.-H. Wang, and Y.-T. Shieh (1996), Dust: A diagnostic of the hydrological cycle during the last glacial maximum, *Science*, *271*, 962–963.
- Zielinski, G. A., and G. R. Mershon (1997), Paleoenvironmental implications of the soluble microparticle record in the GISP2 (Greenland) ice core during the rapidly changing climate of the Pleistocene-Holocene transition, *Geol. Soc. Am. Bull.*, *109*, 547–559.
- Zou, X. K., and P. M. Zhai (2004), Relationship between vegetation coverage and spring dust storms over northern China, *J. Geophys. Res.*, *109*, D03104, doi:10.1029/2003JD003913.
- Zweck, C., and P. Huybrechts (2005), Modeling of the Northern Hemisphere ice sheets during the last glacial cycle and glaciological sensitivity, *J. Geophys. Res.*, *110*, D07103, doi:10.1029/2004JD005489.
-
- H. Fischer and U. Ruth, Alfred Wegener Institute for Polar and Marine Research, Columbusstrasse, D-27568 Bremerhaven, Germany. (hufischer@awi-bremerhaven.de)
- R. Röthlisberger and E. Wolff, British Antarctic Survey, High Cross, Madingley Road, Cambridge CB3 0ET, UK.
- M.-L. Siggaard-Andersen, Niels Bohr Institute, University of Copenhagen, Juliane Maries Vej 30, DK-2100 Copenhagen OE, Denmark.